UHASSELT
KNOWLEDGE IN ACTION

Maastricht University

Faculteit Geneeskunde en Levenswetenschappen
School voor Levenswetenschappen
master in de biomedische wetenschappen

Masterthesis

Comparison of AIRO intraoperative CT with C-arm fluoroscopy during posterior lumbar interbody fusion: safety and clinical efficacy

Gwendolien Smets

Scriptie ingediend tot het behalen van de graad van master in de biomedische wetenschappen, afstudeerrichting klinische moleculaire wetenschappen

PROMOTOR :

Prof. dr. Jan VANDEVENNE

BEGELEIDER :

dr. Sofie VAN CAUTER

2018
2019

De transnationale Universiteit Limburg is een uniek samenwerkingsverband van twee universiteiten in twee landen: de Universiteit Hasselt en Maastricht University.

UHASSELT
KNOWLEDGE IN ACTION

www.uhasselt.be
Universiteit Hasselt
Campus Hasselt:
Martelarenlaan 42 | 3500 Hasselt
Campus Diepenbeek:
Agoralaan Gebouw D | 3590 Diepenbeek

UHASSELT
KNOWLEDGE IN ACTION

Maastricht University

Faculteit Geneeskunde en Levenswetenschappen

School voor Levenswetenschappen

master in de biomedische wetenschappen

Masterthesis

Comparison of AIRO intraoperative CT with C-arm fluoroscopy during posterior lumbar interbody fusion: safety and clinical efficacy

Gwendolien Smets

Scriptie ingediend tot het behalen van de graad van master in de biomedische wetenschappen, afstudeerrichting klinische moleculaire wetenschappen

PROMOTOR :

Prof. dr. Jan VANDEVENNE

BEGELEIDER :

dr. Sofie VAN CAUTER

Acknowledgements

I would like to thank Hasselt university and Ziekenhuizen Oost-Limburg (ZOL) for the opportunity to do clinical research in a multidisciplinary team. I enjoyed my internship very much. Therefore, I would thank all persons involved in this study or internship.

First of all, I would like to say thank you to Prof. dr. Ivo Lambrichts, as my second examiner, for his valuable, constructive comments. He was always able to add that little bit extra to my thesis study. Furthermore, he had faith in me and was a big support to me.

Next, I am grateful to Prof. Dr. Jan Vandevenne, as my principle supervisor, to make it possible for me to conduct this study during my education at Hasselt University. A special thanks to my daily supervisor, Dr. Sofie Van Cauter. I am so grateful for her help, support, constructive comments and most of all to for giving me the opportunity to add an extra clinical part to the study.

This research would not have been possible without the cooperation and motivation of the neurosurgeons, Dr. Eveleen Buelens, Dr. Daenekindt, and Dr. Peuskens. I am also very grateful for the help and support of Dr. Weyns, the nurses in the operating room and the secretaries of the department neurosurgery. Moreover, I am very grateful for all the patients who participated in the study.

A very special thanks to dr. Albrecht Houben, coordinator of radiation protection at ZOL, for helping me understand the physics behind this study, for helping me out with the data analysis, and for providing all the safety measures I needed during surgery. I appreciate everything he has done for me very much.

Furthermore, I would like to thank dr. ir. Inge Thijs and Leentje Dreesen for arranging the administration during my internship, and Robin Bruyndonckx and Stijn Jaspers, from CENSTAT, for helping me out with statistical analysis.

At last, a very special thanks to my friends for their help and support. I am very grateful to have met them and I truly hope this friendship will last for a very long time. And most importantly, a big thank you to my dad, my mom, my brother and his girlfriend, and my boyfriend for supporting me in every possible way. Without their support and faith, I would not have been able to get this far.

Thank you very much!

Content

D

List of Abbreviations

2D	Two-dimensional
3D	Three-dimensional
ALARA	As Low As Reasonably Achievable
BMI	Body Mass Index
CT	Computed Tomography
CTDI	Computed Tomography Dose Index
DAP	Dose Area Product
DLP	Dose Length Product
ED	Effective dose
Gy	Gray
ICRP	International Commission on Radiological Protection
iCT	Intraoperative Computed Tomography
kV	Kilovolt
LIF	Lumbar Interbody Fusion
mA	Milliampere
mAs	Milliampere second
MI-PLIF	Minimally Invasive Posterior Lumbar Interbody Fusion
OR	Operating room
PSD	Peak Skin Dose
ROI	Region of interest
ROS	Reactive oxygen species
SPSS	Statistical Package for Social Sciences
Sv	Sievert

F

Abstract (in English)

Introduction: Instrumented surgeries have evolved over time to more complex minimally invasive procedures, with the help of intraoperative guiding systems based on imaging and navigation. Navigation systems based on imaging have evolved from uniplanar, two-dimensional C-arm fluoroscopy to multiplanar, 3D intraoperative computed tomography (iCT). The purpose of this study is to compare the use of a newly developed navigation system, the AIRO iCT, with the golden standard intraoperative navigation system, C-arm fluoroscopy, during a minimally invasive posterior lumbar interbody fusion. By evaluating radiation exposure of the patient and operating room staff, time-efficiency and clinical efficacy, this study elucidates the advantages and disadvantages of using AIRO iCT during an image-guided instrumented surgery, compared to C-arm fluoroscopy.

Material & methods: A signed informed consent was obtained from every participant, eligible for a full MI-PLIF procedure operated by one of the three neurosurgeons in the Hospital Ziekenhuis Oost-Limburg. The effective dose of the surgeon, operating nurse and anesthesiologist were measured during surgery with personal dosimeters. Furthermore, the effective dose of the patient was calculated and the lateral and abdominal peak skin dose was measured by Gafchromic™ films. Time-efficiency of the surgery was evaluated by recording the duration of pedicle screw fixation and the total operation. The clinical efficacy was assessed by analyzing clinical questionnaires and the number of postoperative days.

Results: A total of 75 patients participated in the study from which 30 patients had surgery with AIRO iCT and 45 with C-arm fluoroscopy. The radiation dose of the surgeon, the operating nurse, and the anesthesiologist was significantly lower with surgeries assisted by iCT, compared to C-arm fluoroscopy. In contrast, the effective dose of the patient significantly increased four times with iCT, compared to C-arm fluoroscopy. However, the lateral peak skin dose of the patient significantly decreased with iCT. Clinical questionnaires show an improvement in pain score, disability score and health state of the patients after six weeks and after a postoperative period of six months to two years, but do not show differences between AIRO iCT and C-arm fluoroscopy.

Conclusion: Using the iCT, radiation exposure of the operating room staff can significantly be reduced. Therefore, it reduces their chance to get a radiation-associated disease. However, iCT increases the effective dose of the patient and prolongs the operative time. Sufficient training should shorten the operative time, and possibly also the effective dose of the patient. Future research must focus on the further evaluation of the long-term clinical efficacy and the cost/benefit ratio of iCT.

H

Abstract (in Dutch)

Introductie: Geïnstrumenteerde chirurgische ingrepen zijn geëvolueerd naar minimaal invasieve ingrepen me behulp van intra-operatieve begeleidingssystemen, gebaseerd op beeldvorming en navigatie. De afgelopen jaren zijn deze navigatiesystemen geëvolueerd van uniplanaire, tweedimensionale C-arm fluoroscopie naar multiplanaire, driedimensionale intra-operatieve computertomografie. In deze studie vergelijken we het gebruik van een nieuw navigatiesysteem, de AIRO intra-operatieve computertomografie (iCT), met de gouden standaard, C-arm fluoroscopie. Door het evalueren van de stralingsblootstelling van de patiënt en het personeel tijdens een geïnstrumenteerde ingreep, de tijd-efficiëntie, en de klinische effectiviteit van de operatie, onthult deze studie de voor- en nadelen van het gebruik van de AIRO iCT t.o.v. C-arm fluoroscopie.

Materiaal en methoden: Een ondertekend informatieformulier werd verzameld van elke studiedeelnemer die in aanmerking kwam voor een volledige posterieure, lumbale, intervertebrale fusie, uitgevoerd door één van de drie neurochirurgen in het ziekenhuis Oost-Limburg te Genk. De effectieve dosis van het aanwezige personeel (chirurg, instrumenterend verpleegkundige en anesthesist) werd gemeten aan de hand van persoonlijke dosimeters. Verder werd de effectieve dosis van de patiënt berekend, en de maximale laterale en abdominale huiddosis van de patiënt werd gemeten aan de hand van Gafchromic™ filmen. De tijd-efficiëntie van de chirurgische ingrepen werd beoordeeld aan de hand van de tijd die nodig was voor het plaatsen van de pedikelschroeven en de totale operatietijd. Ten slotte, werd de klinische effectiviteit van de operaties geëvalueerd aan de hand van klinische vragenlijsten en het aantal postoperatieve dagen.

Resultaten: Er werden 75 patiënten geïncludeerd in de studie, waarvan 30 patiënten geopereerd werden met behulp van de AIRO iCT en 45 met C-arm fluoroscopie. De stralingsdosis van de chirurg, instrumenterend verpleegkundige en de anesthesist is significant lager gedurende operaties met iCT. De effectieve dosis van de patiënt daarentegen, is vier maal hoger met iCT, maar de maximale, laterale huiddosis is significant lager met iCT. Klinische vragenlijsten en parameters toonden een verbetering in de pijn, beperkings- en gezondheidsscore van de patiënten na zes weken, en na een postoperatieve periode van zes maanden tot twee jaar, maar er kon geen verschil waargenomen worden tussen operaties met iCT en C-arm fluoroscopie.

Conclusie: Door gebruik te maken van de iCT, kan de stralingsblootstelling van het opererend personeel sterk verlaagd worden. Het vermindert dus ook de kans op een stralingsgeassocieerde ziekte. Het verhoogt echt wel de effectieve dosis van de patiënt en verlengt de operatieduur. Voldoende training zou moeten zorgen voor een verkorte operatieduur en mogelijks ook een lagere effectieve stralingsdosis van de patiënt. Bijkomend onderzoek moet zich richten op de verdere evaluatie van de klinische effectiviteit op lange termijn en de kosten-batenverhouding van de iCT.

J

1. Introduction

In recent decades, surgical procedures in multiple fields have evolved significantly in order to reduce the operative risk for the patient. Open procedures have evolved to minimally invasive procedures in which smaller incisions are used to minimize muscle retraction and the infection risk and subsequently, shorten the hospitalization period. However, the disadvantage of procedures happening in a more minimally invasive way is the lack of anatomic orientation. This resulted in the technological evolution using medical imaging techniques to guide the surgical procedure (1-3).

Nowadays, image guidance occurs in combination with navigation systems. Navigation systems are intraoperative imaging modalities based on X-rays which guide the surgeon in inserting the surgical instruments in the operation field. Navigation systems have evolved from uniplanar C-arm fluoroscopy generating two-dimensional (2D) images to more advanced multiplanar or three-dimensional (3D) navigation systems. The latest newly developed 3D navigation system is the mobile intraoperative computed tomography (iCT) (1, 3). In this study, the use of C-arm fluoroscopy and iCT during minimally invasive posterior lumbar interbody fusion (MI-PLIF) procedures is compared.

1.1 C-arm fluoroscopy

The current golden standard for intraoperative image-guidance is biplanar C-arm fluoroscopy. C-arm fluoroscopy was one of the first real-time intraoperative imaging modalities. Currently, it is still the most dominant intraoperative imaging modality in spinal procedures (4-6). A fluoroscopy device consists of a mobile unit and a C-arm which contains an X-ray generator, and an X-ray detector in the opposite direction (Figure 1). The C-arm is flexible which enables it to generate radiographic images from different angles (7). However, images can only be obtained in a single plane at a time. If another plane of view is desired, the C-arm must be repositioned or two independent C-arm fluoroscopes must be used simultaneously (1). Typically, two fluoroscopy devices are placed in the lateral and anteroposterior direction to create 2D radiographic images. The additional monitor carts display the generated lateral or anteroposterior image of the region of interest. In this way, the surgeon can orientate the instruments in two different directions, in order to get an indirect 3D image of the area of interest (7).

Figure 1: OEC Fluorostar 7900 series C-arm. *A mobile C-arm contains an X-ray generator and an X-ray detector in the opposite direction. It can create 2D images from different angles. An additional monitor displays the images in real-time (7). 2D: two-dimensional.*

1.2 Intraoperative Computed Tomography

The mobile AIRO iCT, manufactured by Brainlab, is a 3D imaging device that consists of a mobile base that bears a ring and a pedestal. The ring is a CT system, consisting of an X-ray generator and an X-ray detector that can rotate 360 degrees around a gantry. The patient lies on a table fixed to the pedestal in the gantry of the device (Figure 2). When a scan is made, the ring moves over the patient's region of interest while radiographic images from different angles are produced over the total length of the scanned area. As a result, high-resolution 3D images of the entire region of interest are generated (8, 9). Furthermore, the intraoperative CT consists of an extra infrared camera and workstation with navigation software, which allows determining the spatial position and planning of the instruments during surgery (1, 8, 10).

Figure 2: Set-up of the Brainlab AIRO® iCT and a Curve™ neuronavigation system. *The patient is positioned in the center of the CT ring on a surgical table. The camera of the neuronavigation system is placed in front of the iCT scanner. The 3D images of the AIRO are displayed on a dual image monitor (8, 10). iCT: intraoperative computed tomography.*

1.3 Concerns

Several studies have shown that navigation systems are associated with safer and more accurate surgery, compared to freehand surgeries (11-14). However, intraoperative imaging devices almost exclusively use ionizing radiation. As a result, the surgical staff and patients are exposed to this radiation source during every image-guided surgery. While the patient is mainly exposed to the primary beam, the surgeon is exposed to scatter radiation as a result of interaction with the patient. Exposure to ionizing radiation can give rise to several pathologies (6, 15-17). This section discusses the dosimetry, generation, interactions and the biological effects of X-rays. Furthermore, the essential principles and methods in radiation protection are discussed.

1.3.1 Interaction of X-rays with matter

Ionizing radiation is every type of radiation that, in interaction with matter, can cause ionization with energy transfer from the radiation field to the matter. An example is X-radiation (15, 18).

For radiographic imaging, X-rays are produced in the X-ray tube of the imaging device. In the X-ray tube, electrons are produced at the filament by thermionic emission. Thermionic emission involves

the emission of outer-shell electrons as a result of increasing kinetic energy, which is produced by heat. Subsequently, a voltage difference between the cathode and anode accelerates the electrons towards a positively charged target material (e.g. tungsten) in which the electrons lose their kinetic energy by interacting with the atoms of the material. This interaction then leads to the release of a primary beam of X-ray photons, which can interact with the atoms of the patient's body (15, 18).

In the patient's body, the X-ray photons can either be transmitted without interaction, absorbed, or scattered. Two major types of interactions of X-rays with matter play a role in the attenuation of radiologic images during an intervention: Compton scattering and photoelectric absorption. These interactions contribute the most to the radiation dose of patient and staff (Figure 3) (15, 18).

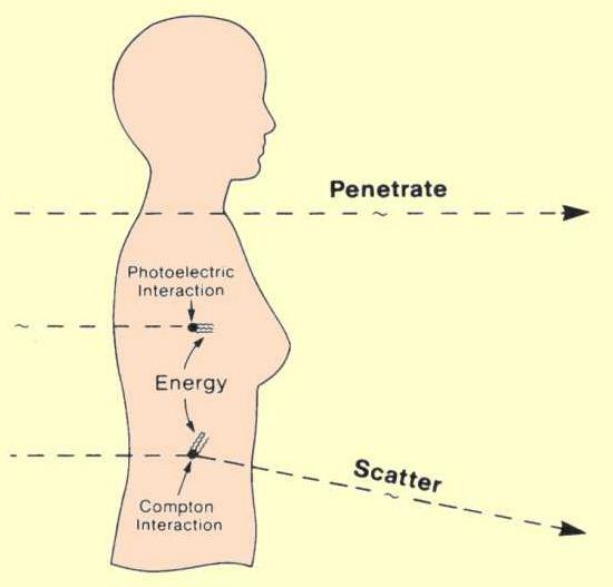

Figure 3: X-ray photon interaction with the human body in diagnostic radiology. *An X-ray photon can interact with the human body in three possible ways: it can penetrate the body without interaction, it can interact with matter and completely be absorbed by depositing its energy, or it can interact and be scattered or deflected from its original direction and deposit part of its energy (Adapted from The physical principles of medical imaging by Perry Sprawls).*

The predominant scatter during a radiologic procedure is Compton scattering. This process mainly occurs when the energy of the incident photon is much larger than the binding energy of the interacting valence-shell electron. During the interaction, energy is transferred from the incident photon to both an electron and an emitting photon. The electron is ejected from the atom, and the scattered photon is emitted with lower energy relative to the initial photon (Figure 4A). The photon may travel in any direction but the electron can only travel in a forward direction relative to the incident photon. Eventually, the secondary electron will lose its kinetic energy through excitation and ionization of another atom in the surrounding tissue. The emitted photon can traverse the tissue without interaction or can undergo new interactions (15, 18).

Photoelectric absorption occurs when the electromagnetic energy of the photon is completely transferred to an inner-shell electron of an atom in the patient's body. When the energy of the photon is bigger than the binding energy of the electron, the electron will be ejected, causing a vacancy in the inner shell of the atom. Consequently, this vacancy will then be filled with an electron of an

orbital further from the nucleus with lower binding energy. This creates another vacancy, which, in turn, is filled by an electron from a shell with an even lower binding energy. Thus, electron jumps from outer- to inner-shells occur (Figure 4B). The energy loss of the jumping electrons produces characteristic radiation. Also here, the ejected electron can excite and ionize atoms in the tissue environment (15, 18).

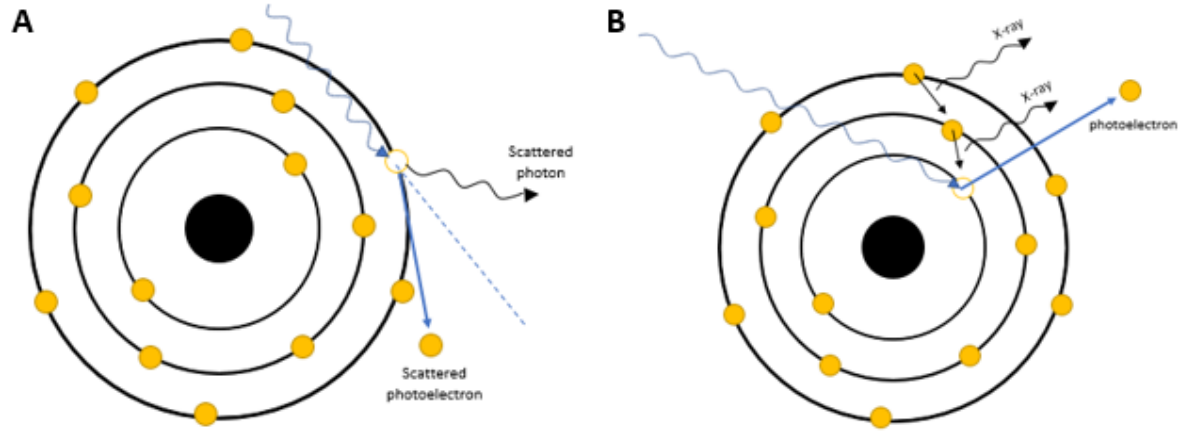

Figure 4: Interaction of X-rays with matter. *A) Compton scattering: an incident photon interacts with a valence-shell electron. As a result, a photoelectron and a photon with lower energy are emitted from the atom. B) Photoelectric absorption: an incident photon interacts with and ejects an inner-shell electron. The subsequent vacancy in the shell is filled with an electron from the upper shell, followed by a series of quantum jumps of electrons towards the nucleus. The difference in binding energy from the jumping electrons is released as characteristic X-rays (15, 18).*

1.3.2 Radiation dosimetry

Radiation doses can be expressed in Gray (Gy) or Sievert (Sv). The absorbed dose of an individual is expressed in Gy. This is the proportion of the average energy transferred by the ionizing radiation as a result of the interaction, to the irradiated mass. The absorbed dose does not take into account the type of radiation (low or high ionization density). The equivalent dose (H_T), in contrast, does account for the type of radiation by multiplying the average absorbed dose ($D_{T,R}$) in tissue or in an organ T as a result of radiation R, with the appropriate radiation weighting factor W_R (e.g. W_R: photons = 1, alpha particles = 20). This dose is expressed in Sv.

$$H_T = \sum w_R D_{T,R}$$

To estimate the potential biological damage, the effective dose (ED) is quantified. This dosage accounts for the differences in sensitivity of tissue to ionizing radiation by introducing a tissue weighting factor (W_T) in the formula (e.g. W_T: gonads = 0,20, lung = 0,12). It represents the stochastic effects of the whole body.

$$ED = \sum w_T H_T$$

To summarize, Gy is used for physical quantification, whether Sv is used to quantify the biological effect of radiation exposure (15, 18).

1.3.3 Exposure to ionizing radiation

As mentioned above, an incident photon can lead to a range of excitations and ionizations in the patient's body. This can cause damage to the important biomolecules (DNA, RNA, proteins) in the human cells. On a molecular level, biomolecules are damaged either directly or indirectly (15, 19). Direct ionization occurs when the incident photon or the lower energy electrons interact with a biomolecule in the cell. However, because the biological cell mainly consists of water (the cytoplasm), damage to biomolecules frequently occurs via reactive oxygen species (ROS), which are formed as a result of the ionization of water molecules. ROS can interact with biomolecules by ionizing them, by disrupting the chemical bonds of the molecule or by the formation of toxic substances. When damage to the essential biomolecule is not repaired, it can give rise to several biological responses (15).

The pathological effects of ionizing radiation can be divided into deterministic and stochastic effects. Deterministic effects are short-term responses, which can only be seen after a specific radiation threshold has been reached. Once the threshold is reached, the severity of the injury increases with the radiation dose (6, 15-17). It is associated with cell killing after high radiation doses, which clinically presents itself in degenerative changes (15). Examples of associated pathologies are hair loss, skin erythema, fibrosis, skin burns, and cataract formation. Since the dose thresholds of deterministic effects are known in many cases, these effects can be prevented by careful monitoring of radiation exposure levels over short time periods (6). Except for prolonged fluoroscopy-guided interventions, the thresholds for deterministic effects are not reached (15). Of greater concern are the stochastic effects (6, 15, 16). These effects are effects that occur by chance. Herewith, the probability of the effect occurring increases with the radiation dose without any definitive time period or specific threshold. It is mostly associated with carcinogenesis and hereditary effects (6, 15-18). Stochastic effects are considered as the principal health risks of low-dose radiation, such as exposures of patient and staff to radiation from diagnostic imaging devices (15).

1.3.4 Radiation protection

Because of the potential harm of radiation, safety measures are important to guide situations where the use of radiation is avoidable or where no alternative can be used. Therefore, the International Commission on Radiological Protection (ICRP) has formulated three main principles that apply to radiation protection. These principles include justification, optimization, and dose limitation. The justification principle claims that the benefit of using radiation for medical purposes must always outweigh the potential harm of the exposure. This does not only apply to the person to be scanned but also to the community. Optimization involves keeping the individual radiation dose "As Low As Reasonably Achievable" (ALARA), taking societal and economic factors into account. This is called the ALARA principle. This principle focuses mostly on the personnel but is also applicable to patients. In medical imaging, this is weighing between good image quality for diagnosis and the administered radiation dose. The third principle states that the total radiation dose of any individual should not exceed appropriate dose limits. For staff, this dose limit is set at 20 mSv in a time span of twelve consecutive months. Herewith, reaching the dose limit can be controlled by wearing personal dosimeters. For the general public, the limit is 1 mSv per year but for medical exposure of patients and emergency situations, no dose limit exists (15, 20, 21).

Furthermore, radiation protection programs describe methods for minimizing the exposure of the medical staff to radiation, following the ALARA principle (16, 21). It includes four main rules: minimize the time spent in the presence of a radiation source, maximize the distance from a radioactive source, maximize shielding between a source and persons, and controlling contamination by radioactive material (6, 15, 16, 21). The time exposure can be reduced by having a clear understanding of the task to be performed and the appropriate equipment to perform them (15, 21). Maximizing the distance from a source is efficient in reducing the radiation dose because radiation follows the inverse square law. This law claims that the dose is lowered with the square of the distance from the radiation or scatter source. Shielding consists of both personal shielding and physical barriers. Physical barriers may be installed in the walls, floor or ceiling of a room, e.g. the operating room (OR), or it can be wrapped around a radiation source. Personal shielding consists of lead aprons, thyroid shields or other protective wearables for radiosensitive areas (6, 15, 21). Lastly, contamination by radioactive materials can be reduced by minimizing the number of radioactive materials in the surrounding (15, 16, 21).

1.4 Lumbar interbody fusions

A lumbar interbody fusion (LIF) is an example of an instrumented spine surgery in which navigation systems are used for orientation of the surgical materials in the patient's body. It is an effective treatment for patients with lumbar spinal disorders in whom symptoms remain unbearable after conservative management (5, 22-24).

A full LIF procedure involves the placement of pedicle screws, rods, and graft cages to restore lordosis, stabilize the spine and fuse the vertebrae in order to decompress the nerves in the lumbar spine region. During the procedure, the spine can be approached via five main directions: posterior, transforaminal, oblique, anterior, and lateral (Figure 5) (5, 23). The approach direction is dependent on the case. For example, the anterior approach is a preferred method to restore lordosis while the posterior approach is preferred for isthmic spondylolisthesis (5).

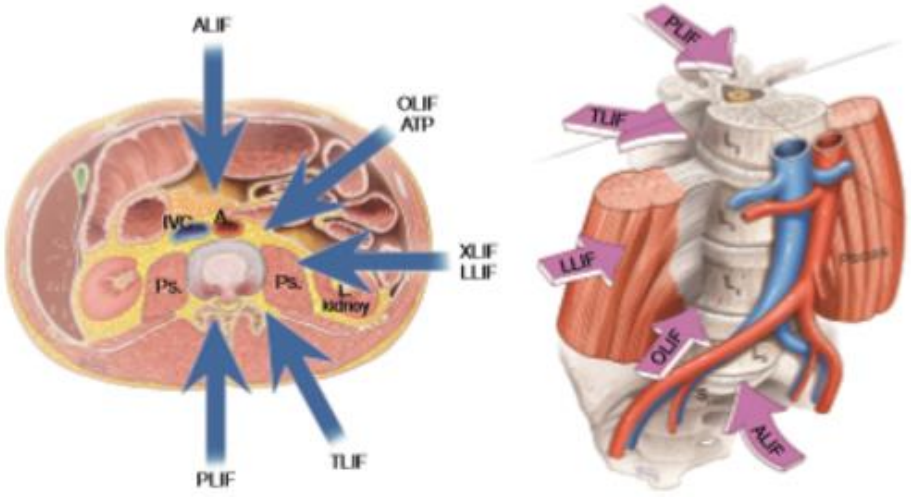

Figure 5: Lumbar interbody fusion: surgical approaches*. The five interbody fusion approaches: anterior (ALIF), lateral or extreme lateral interbody fusion (LLIF or XLIF), oblique lumbar interbody fusion or anterior to psoas (OLIF/ATP), transforaminal (TLIF or MI-TLIF), and posterior (PLIF). The anatomy of the psoas and anterior vasculature determines the approach at various levels. (Adapted from Mobbs et al. (5).)*

All approaches can be performed in a minimally invasive way (5, 23, 24). Minimally invasive techniques involve smaller incisions to achieve surgical fusion. In that way, the destruction of surrounding normal tissue (muscles, joints, and ligaments) in the lumbar spine region is limited (24). This is believed to reduce blood loss, postoperative pain, and disability. It is also associated with faster patient recovery and shorter hospitalization (24-26).

1.4.1 Minimally invasive posterior lumbar intervertebral fusion

Frequently, a traditional posterior approach is used to treat degenerative indications requiring a fusion procedure. During an MI-PLIF procedure, access to the spine is gained from the posterior direction. It allows excellent visualization of the nerve roots and adequate interbody height restoration in order to decompress the nerves. Furthermore, this approach allows a 360-degree fusion through a single incision. Prior to surgery, the patient is positioned in a prone position on the surgical table. During the procedure, pedicle screws and graft cages are implanted in the patient's spine. The pedicles screws are placed via small lateral incisions, in the pedicles of the vertebrae that will be fused. Thereafter, the pedicle screws will be connected with rods. These rods are then manipulated by the surgeon in order to expand the intervertebral space and decompress the nerves, and/or to restore the lordosis of the spine (Figure 6). Next, the spinous process, facet joints and/or laminae are removed through a small midline incision to generate a corridor to the intervertebral disc space. Subsequently, two graft cages are filled with bone fragments of the removed spinous process and placed in the intervertebral space. If possible, additional bone graft material can be placed in the remaining space to increase the surface area for fusion (5).

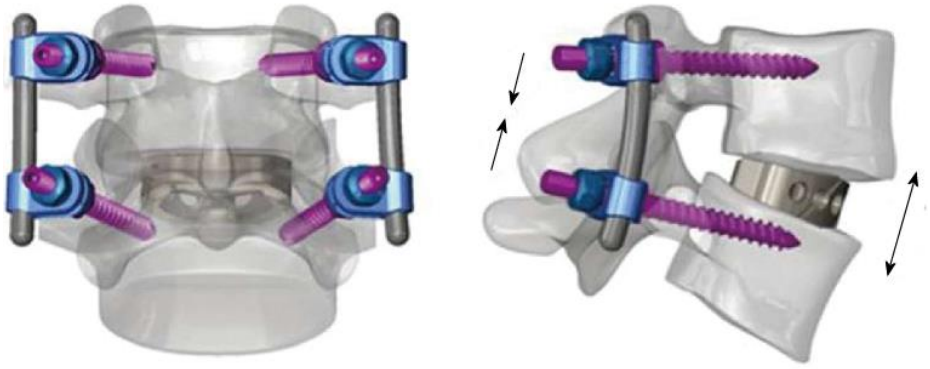

Figure 6: Lumbar interbody fusion: surgical implants. *Pedicle screws are inserted in the upper and lower vertebrae and connected with rods. The screws are then manipulated by the surgeon to restore lordosis. Cages are placed in the intervertebral space between the vertebrae that will be fused. (Adapted from Barrey et al. (27).)*

1.5 The goal of the study

As described above, navigation systems are used to increase the accuracy and safety of instrumentation during minimally invasive surgery. This study evaluates the use of a new, 3D navigation system, the AIRO iCT during an MI-PLIF procedure and compares it to the golden standard technique, C-arm fluoroscopy. The focus is laid on the difference in exposure of the patient and the operating staff to ionizing radiation, and the efficacy of the surgeries assisted by C-arm fluoroscopy or iCT. The hypothesis of our research claims that iCT has an equal or higher radiation dose for the patient, but a lower radiation dose for the operating staff and higher clinical efficacy, compared to

biplanar C-arm fluoroscopy. To test the hypothesis, the peak skin dose (PSD) of the patient and the ED of the patient and the operating staff, during MI-PLIF surgeries assisted by iCT or biplanar C-arms, is quantified. The clinical efficacy of the surgeries is evaluated by the number of postoperative days and clinical questionnaires. Furthermore, also the time-efficiency of both surgeries was evaluated in this study.

The importance of these outcomes is supported by the ALARA-principle which claims that the exposure to radiation must be kept as low as possible to minimize the occurrence of radiation-associated pathologies. It is especially important for surgeons and the operating nurses, who are repetitively exposed to ionizing radiation during surgical procedures, to have knowledge about the radiation dose. Furthermore, knowledge about clinical efficacy is important to outweigh the benefits of the patient with the potential harm of ionizing radiation.

2. Methods

2.1 Patients

Dutch-speaking patients, who underwent a full MI-PLIF surgery with pedicle screw fixation and cage insertion, were asked to participate in the study one day before the surgery from November 2016 until May 2019. Signed informed consent was obtained of every participant. Patients younger than eighteen years old and patients with a fusion of more than two levels were excluded from the study. All surgeries were performed in campus Sint-Jan of Ziekenhuizen Oost-Limburg (ZOL) and were performed by three neurosurgeons (Dr. Eveleen Buelens, Dr. Thomas Daenekindt, and Dr. Dieter Peuskens) who have eleven, sixteen and nineteen years of experience, respectively.

The assistant imaging techniques during the surgery were either biplanar OEC Fluorostar 7900 series C-arms (GE Healthcare, Little Chalfont, UK) or AIRO® iCT (Mobius Imaging, Shirley, Massachusetts, USA) and a lateral OEC Fluorostar 7900 series C-arm (GE Healthcare, Little Chalfont, UK), dependent on the surgeon's choice. Surgeries assisted by any other imaging technique were excluded from the study.

2.2 Radiation dose quantification

In this study, the PSD of the patient and the ED of the patient, surgeon, operating nurse, and the anesthesiologist were measured during MI-PLIF surgeries with iCT or C-arm fluoroscopy.

2.2.1 Radiation exposure of the operating staff

The radiation exposure of the neurosurgeon, anesthesiologist, and operating nurse was quantified by the ED. This dosage was measured using personal dosimeters (DoseAware system, Phillips, The Netherlands). Personal dosimeters were allocated before the start of the surgery and were always positioned on top of the lead apron. After connection of the dosimeter with a computer, the DoseViewer software program provides a dose-time graph. By marking the start and end time of the operation, the Hp(10) value was presented. This value represents an estimate of the radiation dose at 10 mm depth in soft tissue and serves as the ED of the specific staff member.

2.2.2 Radiation exposure of the patient

To evaluate the radiation exposure of the patient, derived from the imaging devices during the surgery, the PSD and the ED of the patient were quantified.

The ED of the patient was calculated by using the parameters of the imaging devices and a conversion factor. The parameters of iCT were collected after each scan and included kilovolt (kV), milliampere (mA), milliampere-second (mAs), computed tomography dose index (CTDI), and dose length product (DLP). Parameters of the lateral C-arm were collected at the end of the surgery. These consisted of kV, mA, dose area product (DAP), entrance dose, and fluoroscopy time. All collected parameters give indirect information about the X-rays and the radiation dose, produced by the devices (Table 1).

Table 1: Collected parameters of the devices and their explanation *(18).*

Parameters	**Explanation**
Kilovolt (kV)	• Potential difference existing between the cathode and anode of an X-ray tube • Measure for the speed of the electrons
Milliampere (mA)	• The current flowing through the X-ray tube • A measure of the number of electrons
Milliampere second (mAs)	• The current flowing through the X-ray tube multiplied by the time (in seconds) • Measure for the number of electrons flowing during acquisition
Dose Length Product (DLP)	• Measure for the radiation dose at the entrance of the skin of the patient, over a specific length
Computed tomography dose index (CTDI)	• The radiation dose of the CT scanner (inclusive scatter radiation)
Dose Area Product (DAP)	• Measures dose over the total irradiated area
Entrance dose	• Measure for the radiation *dose* that is absorbed by the skin as it reaches the patient (including back-scatter)
Fluoroscopy time	• The total length of fluoroscopy

The conversion factor was calculated by a Monte Carlo simulation program. This program computes a 3D dose distribution for a geometrical model of a fictive patient by tracking the trajectory and energy deposition of X-ray photons through the geometrical model (15). Thereafter, the ED, derived from iCT was computed by multiplying the conversion factor with the sum of all collected DLPs during surgery. The ED produced by the lateral C-arm was calculated by multiplying the conversion factor with the entrance dose. Because the placement of the graft cages in the iCT group is assisted by a lateral C-arm, the total ED for these patients was obtained by a summation of the ED of the iCT and the ED of the lateral C-arm.

In order to measure the localized radiation dose on the frontal and lateral skin, the PSD was quantified with Gafchromic™ films. Gafchromic™ films are films that darken when they are exposed to ionizing radiation. This darkening is dependent on the radiation dose to which they are exposed. The films were placed on the frontal and lateral abdomen (side of the X-ray source) of the patient at the level of operation before the patient is positioned for surgery. After surgery, the Gafchromic™ films were scanned together with a calibration matrix of Gafchromic™ films with known dose, in the center of the scan area. By using the region-of-interest (ROI) manager tool of a Fiji Image J software, pixels in the red channel could be converted to a radiation dose in mGy, after fitting the data on the calibration matrix curve with a macro code.

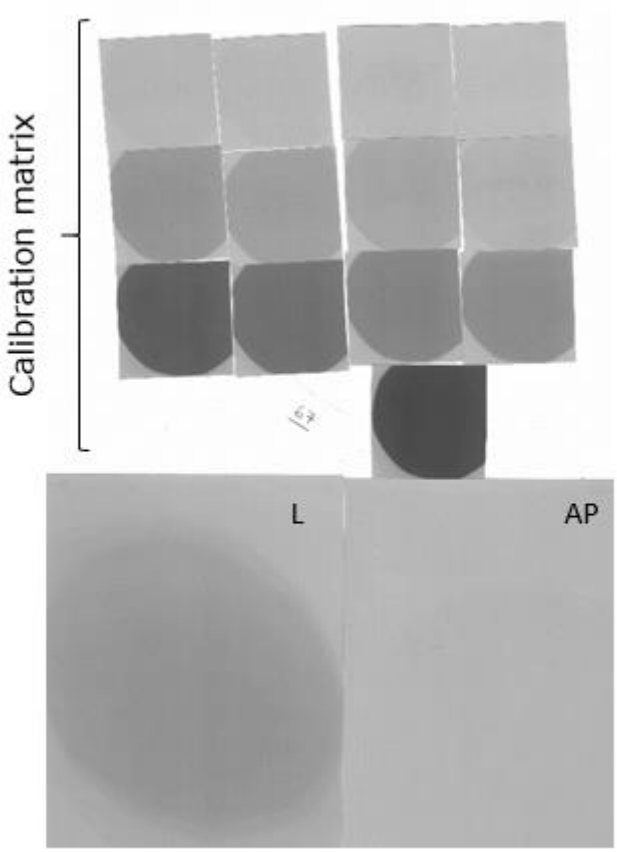

Figure 7: Analysis of a lateral and anteroposterior Gafchromic™ film. *After surgery, the exposed Gafchromic™ films and a calibration matrix are scanned and processed with an Image J program. Measured data are fit on the calibration curve and the corresponding radiation dose in mGy is quantified. AP: anteroposterior film; L: lateral film; mGy: milliGray.*

2.3 Time efficiency

To evaluate the time efficiency of the surgeries, the duration of pedicle screw placement and the total operation time was measured. The total operation time length includes the time between the first incision and the last suture (time interval 2- figure 8). Pedicle screws were inserted prior to decompression and thus this interval was measured from narcosis to decompression (time interval 1- figure 8). During surgeries with AIRO iCT, an iCT scan was made prior to pedicle screw insertion. This scan was used for intraoperative localization and planning of the surgical instruments. When finished, the accuracy of pedicle screw placement was evaluated with a second iCT scan. In contrast, during surgeries with C-arm fluoroscopy, pedicle screw placement was navigated and evaluated by real-time imaging with a lateral-lateral and anteroposterior C-arm fluoroscope. Cage placement was assisted by a lateral C-arm fluoroscope during every MI-PLIF procedure.

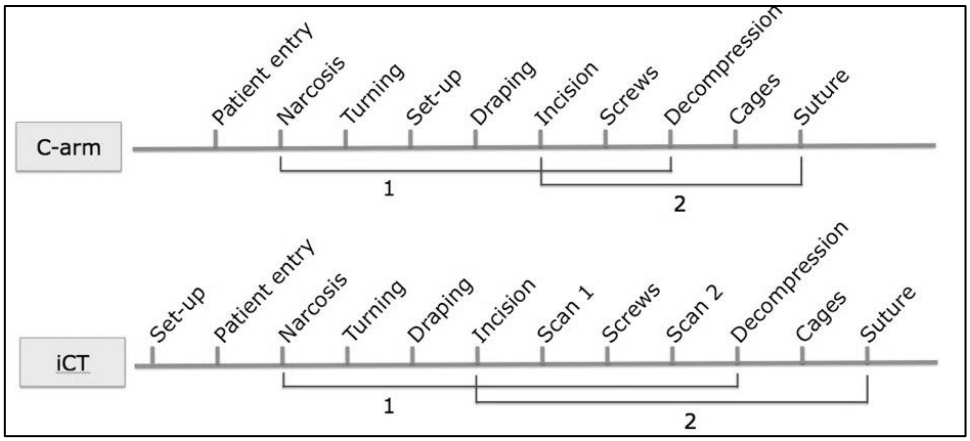

Figure 8: Included workflow steps in the time interval of pedicle screw placement and total operation duration, during MI-PLIF procedures assisted by C-arm fluoroscopy or AIRO iCT. *Time interval 1 represents all included steps for pedicle screw placement between narcosis and decompression, during MI-PLIF procedures with C-arm fluoroscopy or iCT. The included steps are narcosis, (set-up of C-arm fluoroscopes,) turning the patient in the appropriated position for surgery, draping and sterilization of the patient, incision making and screw placement. The time point for the set-up of the imaging devices differs between the surgeries. In iCT-assisted surgeries, the iCT is set-up before patient entry, while with C-arm fluoroscopy the set-up occurs after the patient is turned on the operating table. Time interval 2 includes all required steps between the incision and suture. It includes incision making, pedicle screw placement, decompression, cage placement, and suture. iCT: intraoperative CT. MI-PLIF: minimally invasive posterior lumbar interbody fusion.*

2.4 Clinical efficacy

To investigate whether there is a difference in clinical efficacy between patients operated with the assistance of C-arm fluoroscopy or iCT, patients included between December 2018 and June 2019 were asked to complete a questionnaire before and six weeks after the surgery (prospective). Study participants, operated before December 2018, were asked to complete this questionnaire about their pain, disability and health state before the surgery and their current pain, disability and health state (retrospective). The questionnaire consisted of a numeric visual analog scale (VAS), an Oswestry Disability Index (ODI) questionnaire and a EuroQol- five dimensions- five levels (EQ-5D-5L) questionnaire. A pain score of 0-2, 3-4, 5-6, 7-8 and 9-10 on the VAS was respectively defined as no pain, mild pain, annoying pain, pronounced pain, and unbearable pain. The EQ-5D-5L questionnaire consists of two pages, the descriptive system and an EQ-VAS. The descriptive system comprises five multiple choice questions about the five dimensions of health state (mobility, self-care, daily activities, pain/discomfort, and anxiety/depression). Each question has five levels: no problems, slight problems, moderate problems, severe problems, and extreme problems. However, the wording of these levels is adapted to the dimension, to increase consistency. The patients were asked to indicate the most appropriate level applicable by placing a cross in the box against the most appropriate statement. The EQ VAS records the patient's self-rated health on a 20 cm vertical VAS, ranging from 0% ("the worst health you can imagine") to 100% ("the best health you can imagine"). The patients were asked to rate their general health by placing a cross on the VAS and writing the corresponding number in the box next to it. At last, the ODI score was calculated, using the ODI questionnaire. This questionnaire includes ten questions about the severity of the pain, self-care, lifting, walking, sitting, standing, sleeping, sex life, social life, and traveling/transport. Each question was scored from 0 to 5 based on their respondents. The ODI score (in percentage) was calculated

by the sum of the score per question, multiplied by two. This score gives information about how low back pain and/or leg pain affects the patient's ability to manage in everyday life. A score of 0%-20%, 21%-40%, 41%-60%, 61%-80%, and 81%-100% was respectively defined as minimally disabled, moderately disabled, clearly disabled, very disabled to handicapped, and bed-ridden or exaggerated. In addition to the questionnaires, the number of postoperative days in the hospital was analyzed.

2.5 Statistical analysis

Normally distributed or not-normally distributed, continuous variables are expressed as mean ± SD or as median (interquartile range), respectively. Normality was assessed by the Shapiro-Wilk statistic. To define the difference in unpaired continuous variables (e.g. age, BMI, radiation dose, operation length, number of postoperative hospitalization days, etc.) between both groups, an independent T-test or Mann-Whitney U test were performed, depending on the normality of the data. Differences between unpaired categorical variables (e.g. gender, indications, operator) were assessed by a chi-square or Fishers exact ($n<5$) test. Furthermore, a Spearman's correlation analysis was done to evaluate the correlation between the BMI and the ED of the patient per group. All statistical analyses were performed using the Statistical Package for Social Sciences release 25.0 (IBM®SPSS®Inc., Chicago, Illinois, USA) with a significance level α of 5%.

3. Results

3.1 Demography

There were 100 potential candidates for the study. Of these, 25 were excluded from the study because of the following reasons: incomplete informed consent (n= 9), no full MI-PLIF procedure (n= 9), other LIF procedure (n= 2), other C-arm fluoroscopy used (n= 4) or when more than two levels of vertebrae were fused (n= 1). A total of 75 patients participated in the study. Of these, 30 patients underwent a full MI-PLIF surgery with the assistance of the AIRO CT device, while 45 patients had surgery with the assistance of two C-arm fluoroscopy devices. The iCT group consisted of eleven males and nineteen females with a median BMI of 27 and a median age of 60 years. Similarly, the fluoroscopy group included 21 males and 24 females with a median BMI of 26.5 and a median age of 60 years.

The indications for an MI-PLIF surgery in the iCT group consisted mainly of listhesis (n=16) or a combination of multiple lumbar disorders (n=7). However, some patients in the iCT group were offered a MI-PLIF surgery because of discopathy (n=3), hernia (n=2) and therapy-resistant pain (n=2). The study participants in the C-arm fluoroscopy group had undergone a MI-PLIF surgery because of listhesis (n=16), multiple spinal disorders (n=18), discopathy (n=4), stenosis (n=3), hernia (n=1), facet arthrosis (n=1), or another lumbar spine disorder (n=1). A total of 29 (96.7%) patients in the iCT group had a single-level lumbar spinal fusion. Only one individual had two levels of vertebrae fused (3.3%). On the other hand, 38 (84.4%) patients of the fluoroscopy group had a single-level fusion, while 7 (15.6%) patients had a multi-level fusion. There is no significant difference between both groups in terms of age, BMI, gender, indications, and number of levels to be fused. However, the groups were not comparative in the count of surgeries performed by surgeon 1, 2 or 3. Surgeon 1 performed 20 surgeries (iCT: n= 19; C-arm fluoroscopy; n=2), surgeon 2 operated 18 surgeries (iCT: n= 10; C-arm fluoroscopy; n=9) and surgeon 3 performed 33 surgeries (iCT: n= 1; C-arm fluoroscopy; n=35). A summary of the basic characteristics of the study population in both groups is given in table 2.

Table 2: Basic characteristics of the study population per group. The characteristics were compared between the groups by means of a Mann-Whitney U test or a Chi-square test (α= 0.05). A p-value above 0.05 indicates that there is no significant difference between the groups. A p-value beneath 0.05 indicates that there is a significant difference between the groups for that specific variable.

	AIRO iCT (n= 30)	Biplanar C-arm fluoroscopy (n= 45)	p-value
Age, in years (median [IQR])	58 [56-65]	59 [49-72]	0.701
BMI (median [IQR])	27 [23-30]	26.5 [24.25-30]	0.623
Gender (M/F) (% male)	11/19 (36.7)	21/24 (46.7)	0.391
Indications (no. [% of patients])			0.335
Discopathy	3 [10.0]	4 [8.9]	
Listhesis	16 [53.3]	16 [35.6]	
Stenosis	0 [0.0]	3 [6.7]	
Hernia	2 [6.7]	1 [2.3]	
Therapy-resistant pain	2 [6.7]	1[2.3]	
Facet arthrosis	0 [0.0]	1 [2.2]	
Other	0 [0]	1 [2.2]	
Multiple disorders	7 [23.3]	18 [40.0]	
Level fusion (no. [% of patients])			0.093
Single level	29 [96.7]	38 [84.4]	
Multi-level	1 [3.3]	7 [15.6]	
Surgeon (no. [% of patients])			0.000
Surgeon 1	19 [63.3]	2 [4.4]	
Surgeon 2	10 [33.3]	9 [20.0]	
Surgeon 3	1 [3.3]	34 [75.6]	

F = female; iCT: intraoperative computed tomography; IQR = Interquartile Range; M = male; SD = Standard Deviation.

3.2 Radiation dose of the operating staff

The radiation dose of the neurosurgeon, operating nurse and anesthesiologist was evaluated by assessing the ED via personal dosimeters that were always worn on top of the lead apron during surgery. The median ED of the surgeon is 11.00 (5.00- 42.00) µSv during surgeries with AIRO iCT and 151.00 (77.00- 329.00) µSv with c-arm fluoroscopy. Statistical analysis confirms a significant difference in the surgeon's radiation dose between surgeries with AIRO iCT and C-arm fluoroscopy (Figure 9). In summary, the surgeon is exposed to a thirteenfold lower radiation dose on average when AIRO iCT is used instead of C-arm fluoroscopy.

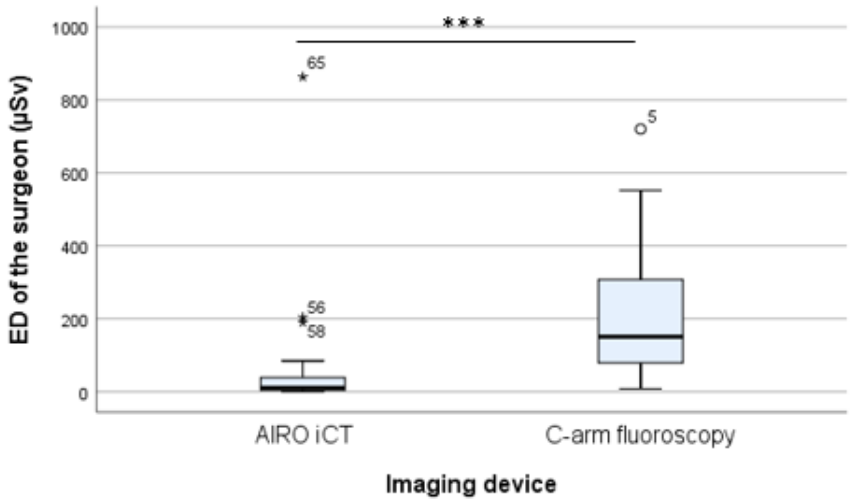

Figure 9: Effective dose of the surgeon during an MI-PLIF procedure. *The ED of the surgeon (in µSv) compared between surgeries assisted by iCT (n=23) or C-arm fluoroscopy (n=41). Data were analyzed by means of a Mann-Whitney U test (***p≤0.001) after testing for normality with a Shapiro-Wilk test. ED: effective dose; iCT: intraoperative computed tomography; MI-PLIF: minimally invasive posterior lumbar interbody fusion; µSv: micro-Sievert.*

Similar to the ED of the surgeon, the ED of the operating nurse is significantly reduced during surgeries with AIRO iCT, compared to C-arm fluoroscopy (Figure 10). The median ED is 2.00 (1.00-6.75) µSv during surgeries with iCT and 8.00 (3.00- 15.25) µSv during surgeries with C-arm fluoroscopy.

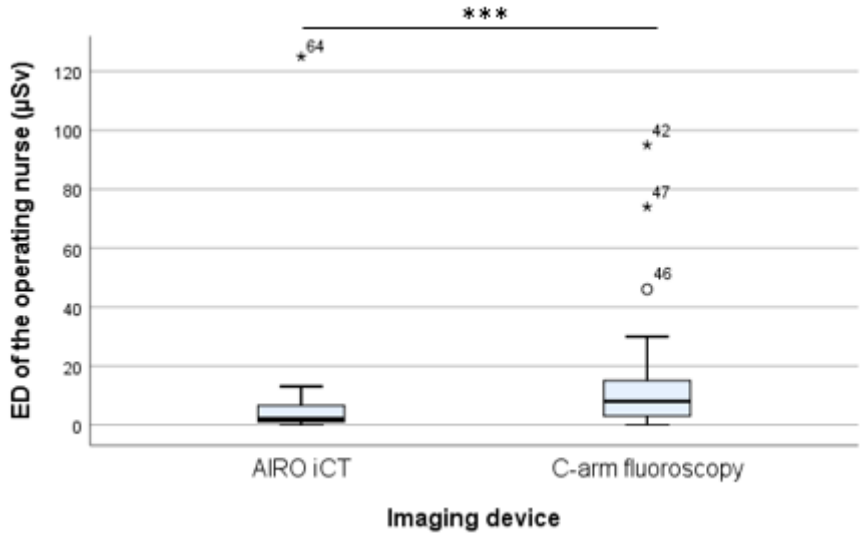

Figure 10: Effective dose of the operating nurse during an MI-PLIF procedure. *The ED of the operating nurse (µSv) compared between surgeries assisted by iCT (n=24) or C-arm fluoroscopy (n=42). Data were analyzed by means of a Mann-Whitney U test (*** p≤0.001) after testing for normality with a Shapiro-Wilk test. ED: effective dose; iCT: intraoperative computed tomography; MI-PLIF: minimally invasive posterior lumbar interbody fusion; µSv: micro-Sievert.*

Furthermore, also the ED of the anesthesiologist was significantly lower during surgeries with iCT, compared to C-arm fluoroscopy (Figure 11). The median ED of the anesthesiologist is 0.00 (0.00- 1.00) µSv with iCT and 1.00 (0.00- 3.00) µSv with C-arm fluoroscopy.

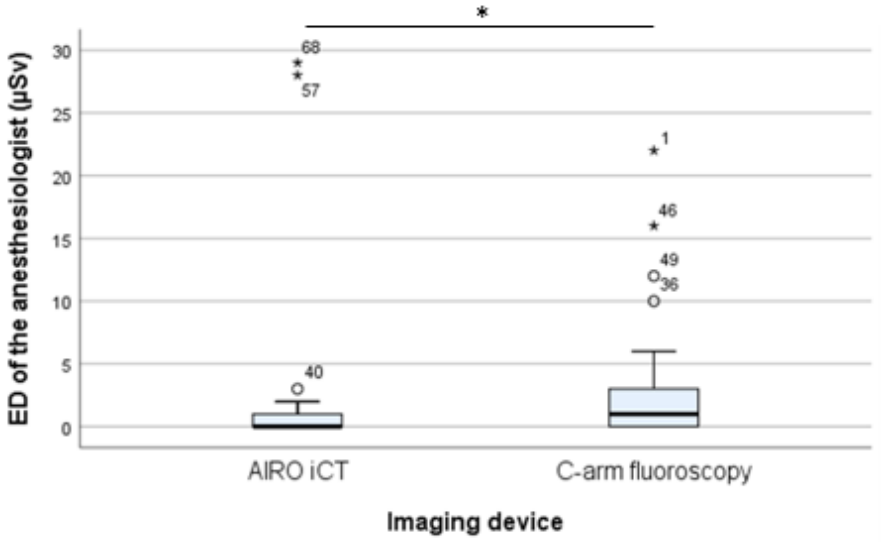

Figure 11: Effective dose of the anesthesiologist during an MI-PLIF procedure. *The ED of the anesthesiologist (µSv) compared between surgeries assisted by iCT (n=24) or C-arm fluoroscopy (n=42). Data were analyzed by means of a Mann-Whitney U test (*p≤0.05) after testing for normality with a Shapiro-Wilk test. ED: effective dose; iCT: intraoperative computed tomography; MI-PLIF: minimally invasive posterior lumbar interbody fusion; µSv: microSievert.*

3.3 Radiation dose of the patient

To evaluate the whole-body dose and the absorbed dose at the abdomen of the patient, the ED, and the lateral and abdominal PSD were quantified, respectively.

3.3.1 Effective dose of the patient

The ED of the patient was calculated using the parameters of the used imaging devices and a conversion factor. Statistical analysis shows a significant difference in the ED of patients operated with AIRO iCT and C-arm fluoroscopy (Figure 12). The median ED during surgeries with AIRO iCT is 8.869 (5.929- 10.639) mSv, while during surgeries with C-arm fluoroscopy the ED of the patient is 2.274 (1.453- 3.472) mSv. Therefore, the median ED of the patient is four times higher during surgery with AIRO iCT, compared to C-arm fluoroscopy.

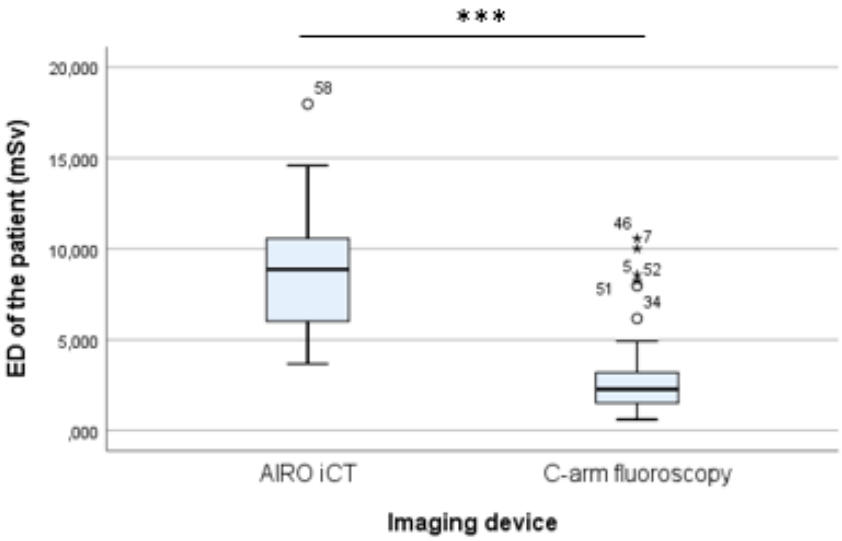

Figure 12: Effective dose of the patient during an MI-PLIF procedure. *The ED of the patient (Sv) compared between surgeries assisted by iCT (n=24) or C-arm fluoroscopy (n=37). Data were analyzed by means of a Mann-Whitney U test (*** p≤0.001) after testing for normality with a Shapiro-Wilk test. ED: effective dose; iCT: intraoperative computed tomography; MI-PLIF: minimally invasive posterior lumbar interbody fusion; mSv: millisievert.*

A Spearman's correlation analysis shows a moderate correlation (r=0.438) between the patient's BMI and the ED of patients who had an MI-PLIF surgery performed with AIRO iCT. However, for patients who had an MI-PLIF with C-arm fluoroscopy, the correlation is only very weak (r=0.071) (Figure 13).

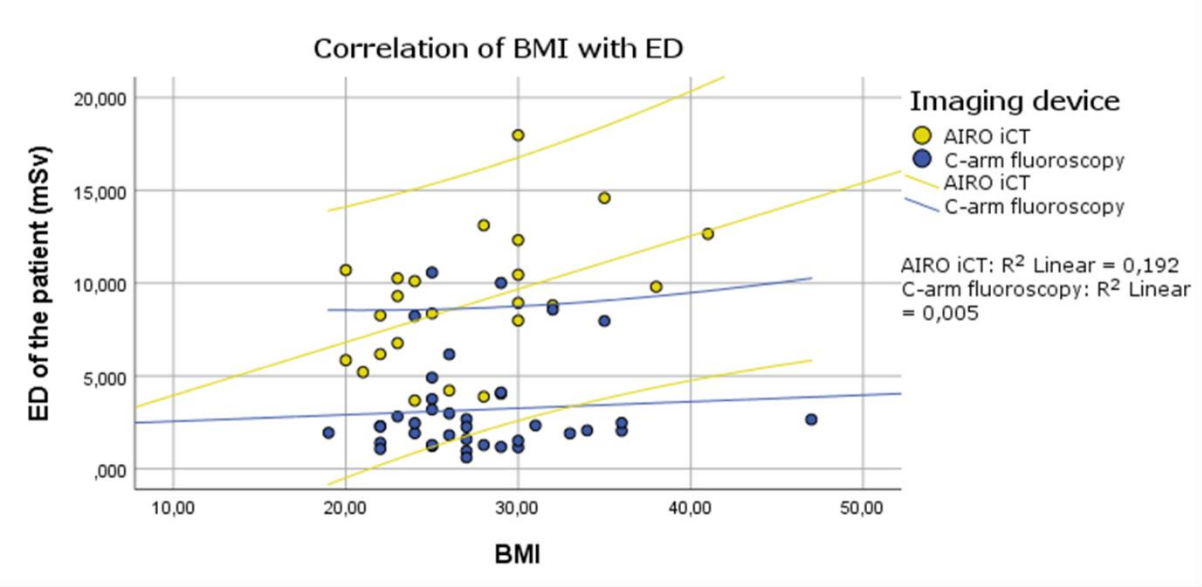

Figure 13: Spearman's correlation between BMI and the effective dose of the patient. *Correlation analysis of the BMI and the ED of patients who had an MI-PLIF surgery assisted by AIRO iCT (n= 24) (R^2=0.192, p<0.05) or C-arm fluoroscopy (n=37) (R^2= 0.005, p>0.05). The lines delineate a 95% confidence interval per subgroup. Data were analyzed with a Spearman's correlation. BMI: body mass index; ED: effective dose; iCT: intraoperative computed tomography.*

3.3.2 Lateral and abdominal peak skin dose

In contrast to the ED of the patient, the localized radiation dose at the lateral abdomen of the patient is significantly higher during surgeries with C-arm fluoroscopy, compared to AIRO iCT (Figure 14A). The median lateral PSD of the patient is 70.354 (49.056- 96.490) mGy with AIRO iCT and 154.150 (96.601- 235.142) mGy with C-arm fluoroscopy. Thus, the lateral PSD of the patients decreases approximately two times when AIRO iCT is used instead of C-arm fluoroscopy. However, the abdominal PSD is lower with both imaging devices and does not differ significantly between surgeries with AIRO iCT and C-arm fluoroscopy (Figure 14B). The median abdominal PSD of the patient ranges between 44.524 (37.973- 59.103) mGy with AIRO iCT and 46.347 (19.972- 65.721) mGy with C-arm fluoroscopy.

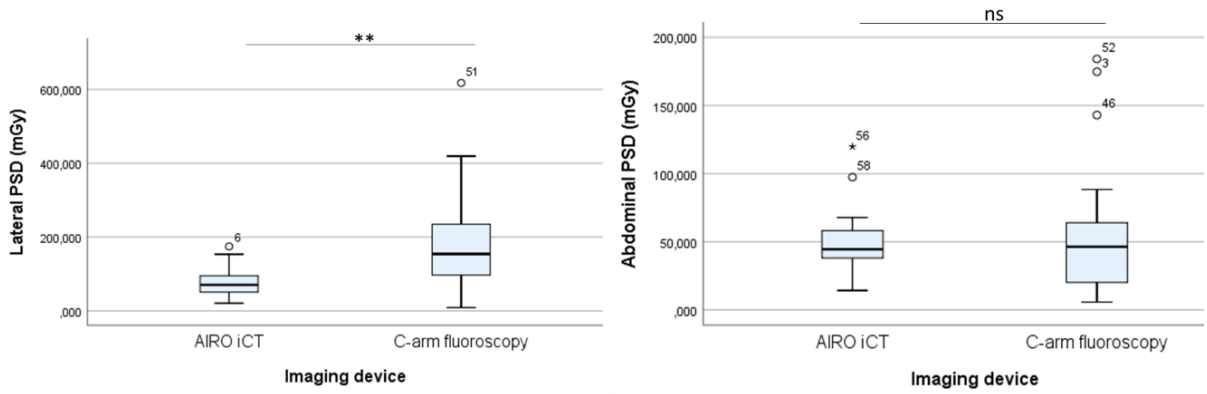

Figure 14: Peak skin dose of the patient during an MI-PLIF procedure. *A) The lateral peak skin dose of the patient (mGy) compared between surgeries assisted by iCT (n=24) or C-arm fluoroscopy (n=27). B) The abdominal peak skin dose of the patient (mGv) compared between surgeries assisted by iCT (n=24) or C-arm fluoroscopy (n=28). Data were analyzed by means of a Mann-Whitney U test after testing for normality with a Shapiro-Wilk test (** p≤0.01) (ns: not significant). iCT: intraoperative computed tomography; MI-PLIF: minimally invasive posterior lumbar interbody fusion; mGy: milliGray; PSD: peak skin dose.*

3.4 Time-efficiency

In order to evaluate the time-efficiency of MI-PLIF surgeries performed by the assistance of C-arm fluoroscopy or AIRO iCT, the total operation length and the duration of pedicle screw insertion was assessed. The median time length for pedicle screw placement and the total operation (in hours:minutes:seconds) is 02:01:41 (1:47:59- 2:41:03) and 03:46:31 (3:22:35- 04:29:20) with AIRO iCT, and 1:20:10 (01:02:45- 01:45:52) and 2:16:00 (1:52:02- 03:01:06). with C-arm fluoroscopy, respectively. In general, pedicle screw insertion prolongs approximately 42 minutes longer on average during surgeries performed with the assistance of iCT, compared to C-arm fluoroscopy and the total operation lasts circa 90 minutes longer on average with iCT. Statistical analysis confirms a significant difference in time-efficiency between MI-PLIF surgeries assisted by AIRO iCT and C-arm fluoroscopy (Figure 15).

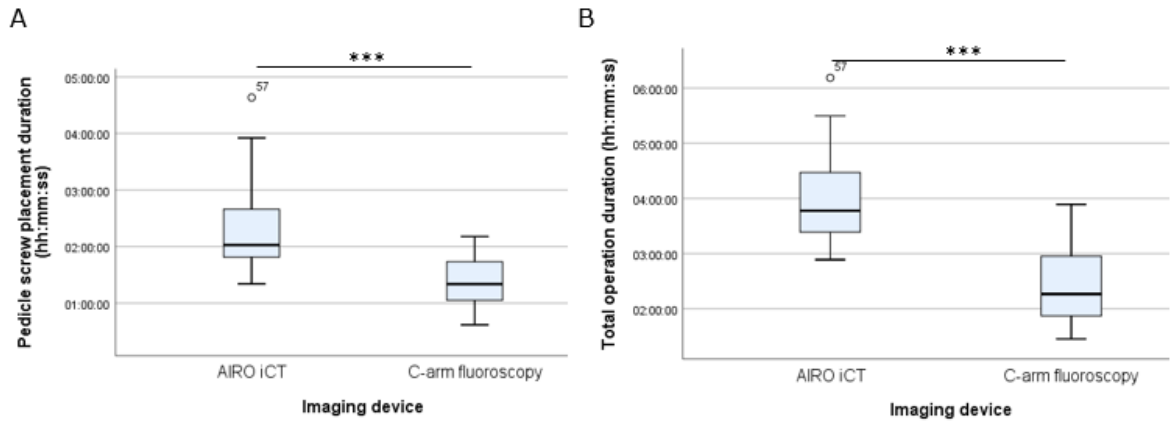

Figure 15: Time efficiency of an MI-PLIF surgery. *A) Duration of pedicle screw insertion (in hh:mm:ss) compared between surgeries assisted by AIRO iCT (n=24) and C-arm fluoroscopy (n=18). B) Total operation duration (in hh:mm:ss) compared between surgeries assisted by AIRO iCT (n=29) and C-arm fluoroscopy (n=43). Data were analyzed by means of a Mann-Whitney U test (*** p≤0.001) after testing for normality with a Shapiro-Wilk test. hh:mm:ss: hours:minutes:seconds; iCT: intraoperative computed tomography;. MI-PLIF: minimally invasive posterior lumbar interbody fusion;*

3.5 Clinical efficacy

To investigate whether the use of AIRO iCT, instead of C-arm fluoroscopy has an influence on the clinical efficacy of the surgery, the study participants were asked to complete a pain scale, an EQ-5D-5L questionnaire, and an ODI questionnaire. Statistical analysis shows no significant difference between both groups in terms of improvement in pain, disability and health score of patients after six postoperative weeks. The improvements in pain and ODI score are represented in figure 16. Analysis of the EQ-5D-5L questionnaire shows improvement of the patients' health state, after six postoperative weeks (figure 17). Similar results were found for patients who completed the questionnaires six months to two years after surgery (supplementary figure 1 and 2).

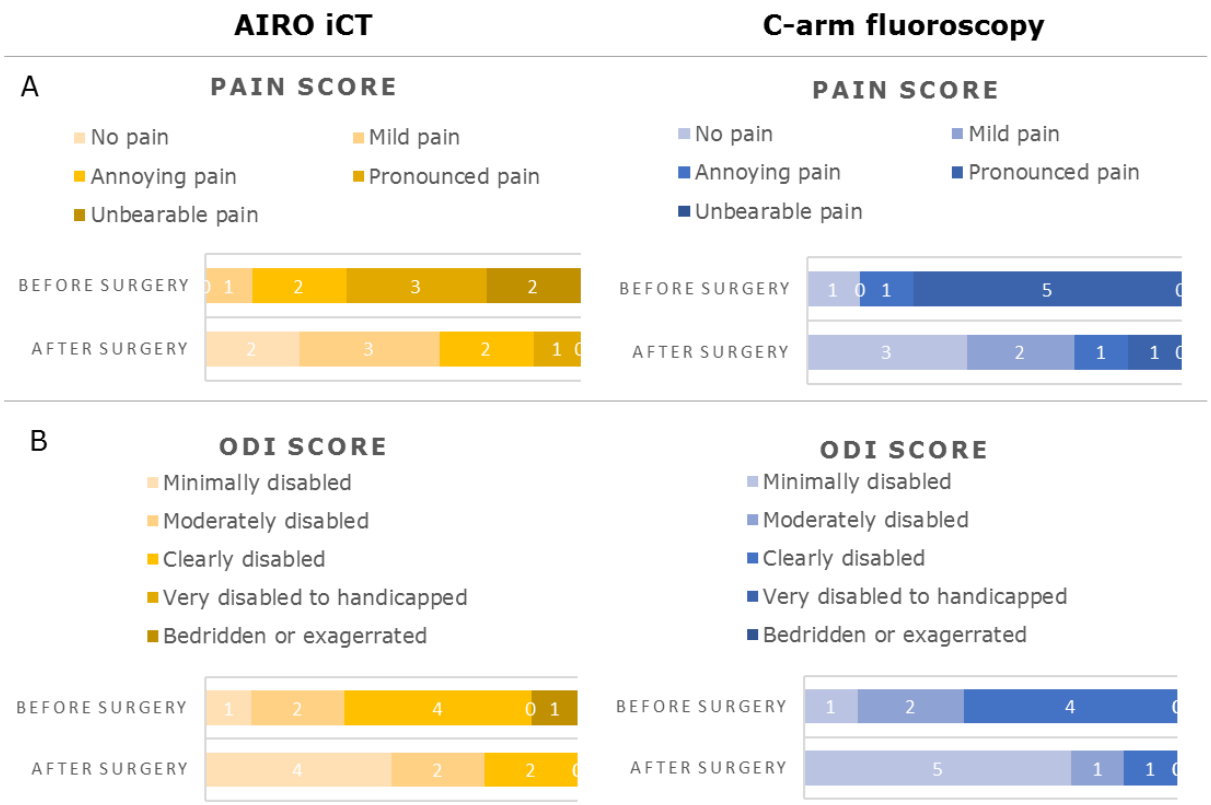

Figure 16: Pain and disability score after six postoperative weeks. *A) Pain degree of the study participants before surgery and six weeks after surgery with AIRO iCT (left) (n=8) or C-arm fluoroscopy (right) (n=7). Data were obtained by a numeric visual analog scale. B) ODI score of the study participants before surgery and six weeks after surgery with AIRO iCT (left) (n=8) or C-arm fluoroscopy (right) (n=7). Data was obtained by an ODI questionnaire. iCT: intraoperative computed tomography; ODI = Oswestry disability index.*

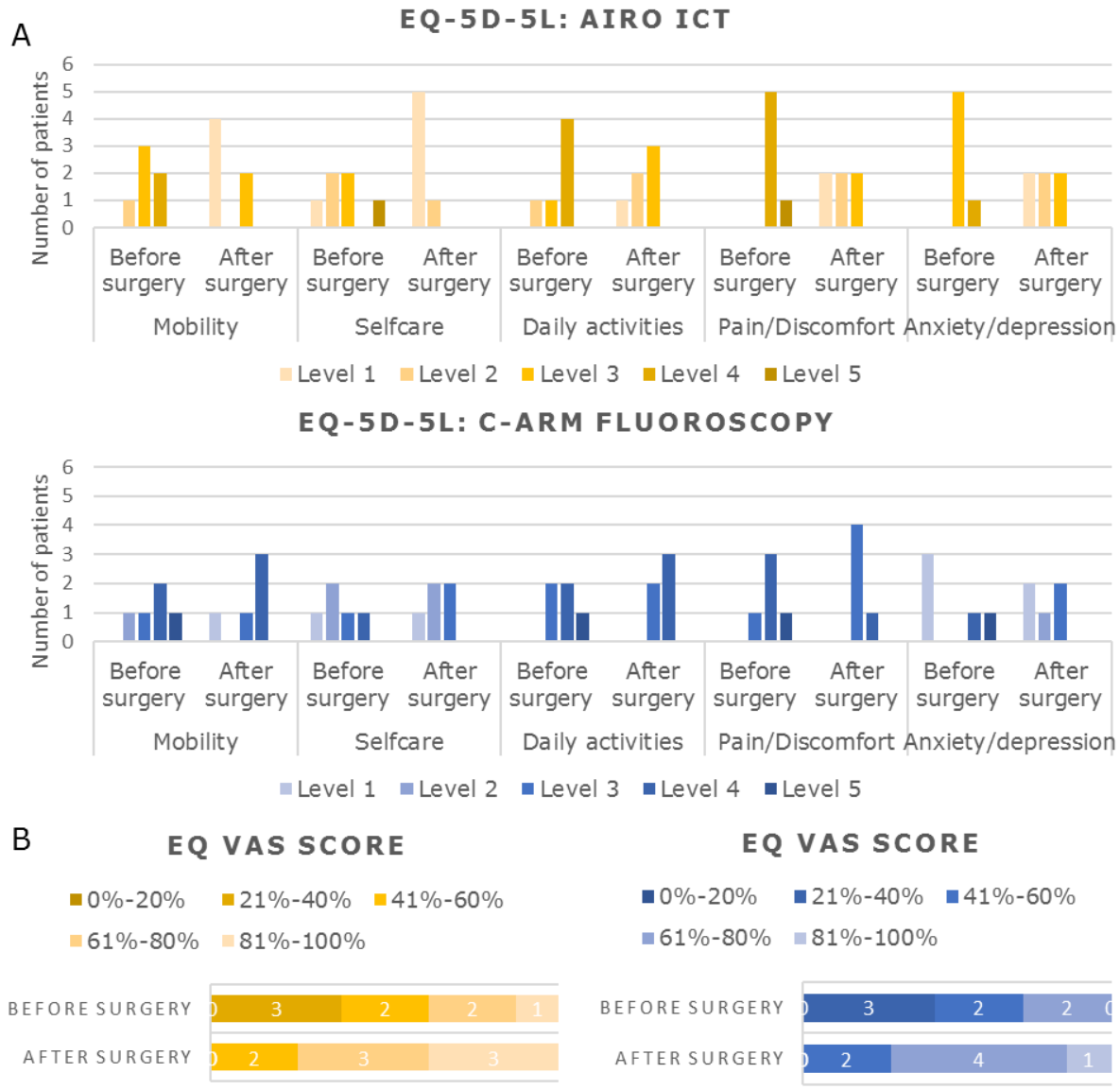

Figure 17: Health state score after six postoperative weeks. *The health state of the study participants was evaluated before the surgery and after six postoperative weeks with an EQ-5D-5L questionnaire and an EQ-VAS. A) Scoring of the five dimensions of health state (mobility, self-care, daily activities, pain/discomfort, and anxiety/depression) before and after surgery with iCT (yellow) (n=8) or C-arm fluoroscopy (blue) (n=7). Level 1= no problems or no pain/discomfort, anxiety/depression, Level 2= mild problems or mild pain/discomfort, anxiety/depression, Level 3= Moderated problems or moderate pain/discomfort, anxiety/depression, Level 4= severe problems or severe pain/discomfort, anxiety/depression, Level 5= extreme problems or extreme pain/discomfort, anxiety /depression. B) The self-rated health score of the study patients before and after surgery with AIRO iCT (left) (n=8) or C-arm fluoroscopy (right) (n=7). EQ-5D-5L: EuroQol- five dimensions- 5 levels; iCT: intraoperative computed tomography; VAS: visual analog scale.*

At last, the number of recovery days was analyzed per group. The median number of postoperative days in the hospital was 5 (4- 6) days including the day of surgery for both study groups. Statistical analysis confirms a nonsignificant difference (Figure 18).

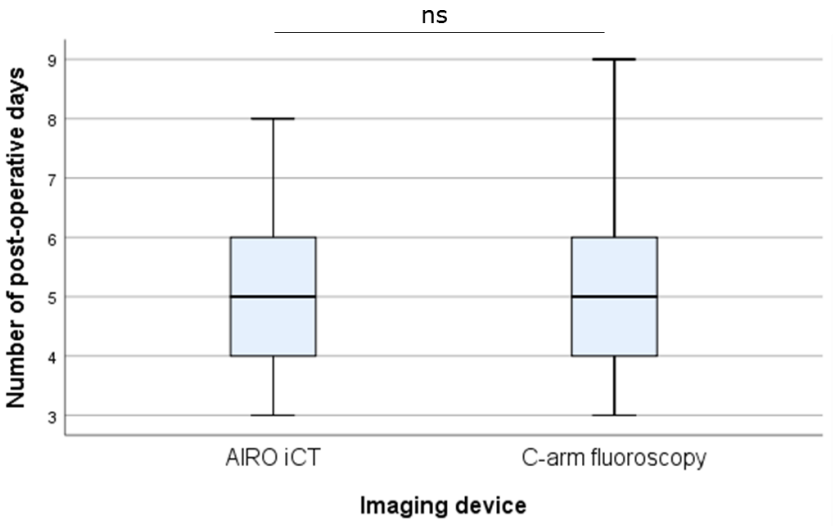

Figure 18: Number of postoperative days. *The number of recovery days that the study patients stayed in the hospital after an MI-PLIF surgery with AIRO iCT (n=22) or C-arm fluoroscopy (n=25) (including the day of surgery). Data were analyzed by means of a Mann-Whitney U test (ns: not significant) after testing for normality with a Shapiro-Wilk test. iCT: intraoperative computed tomography.*

4. Discussion

Over the past decades, navigation systems have evolved from 2D conventional C-arm fluoroscopy to intraoperative 3D imaging. The AIRO iCT is one of the newest 3D imaging devices with navigation.

Knowledge about radiation exposure to the operating staff is of great importance since the long-term effects of chronic low-dose exposure are still unclear (28-31). Our study results show a significant decrease in the ED of the neurosurgeon, the operating nurse, and the anesthesiologist during surgeries performed with iCT, compared to C-arm fluoroscopy. The surgeon's and the operating nurse's radiation dose respectively decreased thirteen and four times on average, while the radiation dose of the anesthesiologist was almost eliminated with iCT. This can be explained by the ability to insert the pedicle screw using a single iCT scan and spinal navigation (6, 8, 15, 21). Prior to pedicle screw insertion, an iCT scan was controlled via a compact system pendant which could be held by an unsterile nurse behind a lead wall in de OR. The sterile surgeon and operating nurse also stood behind this lead wall. Other operating staff, including the anesthesiologist, went outside the OR while scanning. The generated image was then, together with navigation software, used to insert the screw in an accurate manner. Afterward, a second iCT scan was obtained to evaluate the placement of the pedicle screws. If misplaced, the inaccurate screw(s) were relocated and, if in doubt, a third iCT scan was made. In contrast, fluoroscopy-guided surgeries require real-time imaging of the surgical instruments in the region of interest (7). Herewith, the surgeon and operating nurse stand at the contralateral side of the X-ray source when radiographic images are made, resulting in a higher radiation dose. The anesthesiologist is further removed from the operative field during surgery and is therefore exposed to less scatter radiation than the surgeon and the operating nurse. During MI-PLIF surgeries assisted by iCT, an additional lateral C-arm fluoroscopy device was used to guide the insertion of a graft cage in the intervertebral space. Therefore, we believe that the ED of the staff members is mainly due to radiation exposure derived from the lateral C-arm fluoroscope. This thought is supported by Lian *et al.* who could demonstrate that the radiation dose of the OR personnel could be completely eliminated during minimally invasive transforaminal LIF procedures guided by only an AIRO iCT device and 3D navigation (32). In addition, Navarro-Ramirez *et al.* demonstrated that various spinal procedures can be performed with only iCT-navigation, eliminating the use of a C-arm fluoroscope in 75% of the cases (33). The greater interquartile range of surgeries performed with C-arm fluoroscopy, compared to iCT, suggest that the exposure of the OR staff is dependent on the surgeon's experience and the complexity of the surgery, while the radiation output of the iCT is more standardized.

Thus, AIRO iCT-based spinal instrumentation increases the safety of the OR personnel by decreasing or even eliminating radiation exposure. Consequently, surgeons can perform more image-guided surgeries per year when they use iCT, before they reach the annual dose limit of 20 mSv. In addition, it is not necessary to wear a lead skirt during iCT-navigated surgery, since the OR personal can leave the room while scanning (33, 34). Therefore, it can increase ergonomics by avoiding back pain or muscular fatigue caused by the weight of the lead shield after long-lasting procedures (35).

In contrary to the ED of the operating staff, the ED of the patient increased approximately four times on average during surgeries with AIRO iCT, compared to surgeries performed with C-arm fluoroscopy. The rotation and movement of the AIRO iCT cause a more widespread irradiated area, while the

primary radiation bundle of the fluoroscopy device irradiates a more localized area. This also explains why the lateral PSD is higher during surgeries with biplanar C-arm fluoroscopy than with AIRO iCT. The abdominal Gafchromic™ film was only exposed to radiation during pedicle screw fixation, while the lateral Gafchromic™ film was exposed during pedicle screw and cage placement. Therefore, the abdominal PSD is relatively low and does not differ between surgeries with iCT or C-arm fluoroscopy. Bindal *et al.* reported a median anteroposterior skin dose of the patient of 59.5 (8.3- 252) mGy and a lateral skin exposure of 78.8 mGy (6.3- 269.5 mGy) during fluoroscopy-guided transforaminal LIF procedures (36). In comparison to our results, this a slightly higher anteroposterior skin dose and a halved lateral skin dose. However, in their study, no graft cages were inserted with fluoroscopy-guidance.

Even though the ED of the patient is higher with iCT, a postoperative CT scan was not required anymore unless desired by the neurosurgeon. Moreover, it is stated that there is no need to consistently evaluate the placement of the pedicle screws with a second iCT scan since the accuracy is even higher with iCT navigation than with C-arm fluoroscopy (34, 37). Furthermore, there is a moderate positive correlation between the BMI and the ED of the patient during surgeries with iCT. This results from a personalized scan protocol in which the radiation dose is determined on the basis of the age, height, weight and surgery level of the patient. Furthermore, the surgeon can choose to use the full proposed dose, to halve the proposed radiation dose or to minimize the radiation output to 25% of the proposed radiation dose (8). This choice often depends on how corpulent the patient is since abdominal fat is negatively correlated with image quality (38, 39). In contrast, a C-arm fluoroscope only contains a low, medium and a high dose mode which can be selected to adapt image quality. However, the radiation output of a C-arm fluoroscope is mainly dependent on the fluoroscopy time which is controlled by the surgeon and might be biased by the surgeon's experience or the complexity of the case (7).

Surgeries performed with AIRO iCT lasted approximately 90 minutes longer on average than MI-PLIF procedures performed with C-arm fluoroscopy, including an average of 42 extra minutes for intubation, patient positioning and the insertion of pedicle screws. Similarly, Hecht *et al.* reported 30-50 minutes additional time for AIRO iCT set-up and navigated instrumentation, including 18-34 minutes extra surgical time with iCT navigation (34). A meta-analysis, comparing computer-assisted and fluoroscopy-guided surgery confirms a longer total operative time but reported a reduced thoracic pedicle screw insertion time, compared to fluoroscopy-guided surgeries (40). Several factors, associated with iCT, can increase the duration of the surgery. First, AIRO iCT is a newly developed technique and is associated with a steep learning curve (34). In contrast, surgeons are experienced in using C-arm fluoroscopy as the golden standard during image-guided surgeries. Although reports, investigating the learning curve of AIRO iCT are sparse, it has been hypothesized that surgeons with image-guidance skills merely need five cases to obtain sufficient experience with iCT. Furthermore, routine use of iCT and spinal navigation is required to overcome the learning curve (34, 41). During this research, AIRO iCT was not routinely used by the three neurosurgeons. Other possible influencing factors are disruption or interference with the navigation signal caused by bloodstains on the reflective markers or lightning of the surgery lamp. Retightening and recalibration after loosening of the navigation markers also occurred. A new iCT scan was needed if the reference array for navigation loosened or moved, to assure accurate navigation (33). Decreasing the operative

time is desirable because the infection risk is positively correlated with the duration of the surgery (42). However, during this research, no cases of wound infection were encountered.

Comparison of clinical data, before and six weeks after surgery, showed a lower pain and disability score and a better health state of patients who underwent an MI-PLIF surgery with either iCT or fluoroscopy. A significant difference in clinical outcome between surgeries with AIRO iCT or C-arm fluoroscopy was not found. A difference in clinical outcome after six months to two years and in the number of postoperative days was also not found. However, many reports describe higher accuracy of pedicle screw placement during 3D navigated surgeries, compared to fluoroscopy-guided surgeries (13, 40, 43). Hecht *et al.* found a 4 % pedicle screw misplacement rate during 23 consecutive posterior spinal instrumentation surgeries with AIRO iCT (34). Furthermore, Rajasekaran *et al.* could confirm a pedicle screw insertion accuracy rate of 96.2 % during AIRO iCT-navigated spinal deformity surgeries. These findings are in line with Noriega *et al*. who showed a reduction in the percentage of malpositioned screws from 10.3 % to 3.6 % when AIRO was used instead of conventional C-arm fluoroscopy (44). The lower rates are due to the 3D spatial feedback associated with 3D navigation systems and the possibility of direct navigated revision when needed (34, 39, 40). Moreover, A meta-analysis of Meng *et al.* reports a lower malposition rate, less intraoperative blood loss, and fewer complications with computer-assisted surgeries, compared to fluoroscopy-guided surgery (40). Because of these beneficial findings, a difference in clinical efficacy is expected (39). However, we could not demonstrate this in our study to date.

This study has some limitations. First of all, it was conducted by three independent students of Hasselt university which may have caused slight differences in data collection, analysis, and processing. Additionally, there was a significant difference between the iCT and the C-arm fluoroscopy group in terms of the operator who performed the MI-PLIF procedures. Surgeon 1 mainly performed MI-PLIF procedures with iCT, while surgeon 3 only did one surgery with iCT. Since the surgeons have unequal experience, it might have biased our group results. The AIRO iCT and spinal navigation present itself with limitations. Bugs in the software of the device sometimes caused the need to restart the AIRO iCT device during surgery. Furthermore, OR personnel often had difficulties with calibration steps or scanning because of insufficient training, after a software update. These events prolonged the surgery time. At last, actual conclusions about the clinical efficacy on the long-term could not be made since the group sizes were too small to do statistical analysis. Therefore, the potential benefit of iCT-navigated surgeries might not have been fully elucidated.

If the learning curve of AIRO iCT has overcome, iCT-navigation will allow more complex surgeries with improved safety and comfort to the OR personnel and higher pedicle screw fixation accuracy. It promises a long-term benefit for the OR personnel by significantly decreasing radiation exposure and the chance to get a radiation-associated disease. However, the long-term benefit of higher pedicle screw accuracy to the patient must be investigated yet. In order to implement this new technology, the cost/benefit ratio of iCT must be discussed and compared to other 3D navigation systems. Navigation systems are associated with higher costs than fluoroscopes. Therefore, the benefits must

outweigh these costs on the long-term. The possible benefits of 3D navigation that increase cost-efficiency might be defined as fewer revisions, reduced operative time, and more flexible planning of the OR schedule through its mobility. Thus, future research must prove which technology has the best cost/benefit ratio (33, 34).

5. Conclusion

Intraoperative spinal image guidance has evolved rapidly over time. The mobile iCT offers increased safety and comfort to the OR personnel, compared to conventional C-arm fluoroscopy. It promises a long-term benefit for the OR personnel by significantly decreasing radiation exposure and the chance to get a radiation-associated disease. However, this research shows a significantly higher ED of the patient and longer pedicle screw insertion time during AIRO iCT-assisted MI-PLIFs. Sufficient training of the OR staff is needed to overcome the learning curve of iCT in order to reduce the surgical time and to eliminate the second scan for evaluation A difference in clinical efficacy was not found. Since a long-term benefit of AIRO iCT-navigated surgeries is expected because of higher pedicle screw accuracy, further research is needed to investigate differences in clinical outcome, complications, and number of revisions. Furthermore, in order for the AIRO iCT to be implemented, a cost-benefit analysis of AIRO iCT must point out if AIRO iCT is the best 3D navigation technology.

References

1. Holly LT. Image-guided spinal surgery. The international journal of medical robotics + computer assisted surgery : MRCAS. 2006;2(1):7-15.
2. Mezger U, Jendrewski C, Bartels M. Navigation in surgery. Langenbeck's archives of surgery. 2013;398(4):501-14.
3. Overley SC, Cho SK, Mehta AI, Arnold PM. Navigation and Robotics in Spinal Surgery: Where Are We Now? Neurosurgery. 2017;80(3S):S86-S99.
4. Kotsianos D, Wirth S, Fischer T, Euler E, Rock C, Linsenmaier U, et al. 3D imaging with an isocentric mobile C-arm - Comparison of image quality with spiral CT2004. 1590-5 p.
5. Mobbs RJ, Phan K, Malham G, Seex K, Rao PJ. Lumbar interbody fusion: techniques, indications and comparison of interbody fusion options including PLIF, TLIF, MI-TLIF, OLIF/ATP, LLIF and ALIF. Journal of spine surgery (Hong Kong). 2015;1(1):2-18.
6. Narain AS, Hijji FY, Yom KH, Kudaravalli KT, Haws BE, Singh K. Radiation exposure and reduction in the operating room: Perspectives and future directions in spine surgery. World Journal of Orthopedics. 2017;8(7):524-30.
7. Healthcare G. OEC Fluorostar Mobile digital C-arm: Operator manual. In: UT, editor. USA2015.
8. Airo mobile intraoperative CT. Brainlab; 2017.
9. Rajasekaran S, Bhushan M, Aiyer S, Kanna R, Shetty AP. Accuracy of pedicle screw insertion by AIRO((R)) intraoperative CT in complex spinal deformity assessed by a new classification based on technical complexity of screw insertion. European spine journal : official publication of the European Spine Society, the European Spinal Deformity Society, and the European Section of the Cervical Spine Research Society. 2018;27(9):2339-47.
10. Spine navigation. Brainlab; 2017.
11. Jin M, Liu Z, Qiu Y, Yan H, Han X, Zhu Z. Incidence and risk factors for the misplacement of pedicle screws in scoliosis surgery assisted by O-arm navigation-analysis of a large series of one thousand, one hundred and forty five screws. International orthopaedics. 2017;41(4):773-80.
12. Luo TD, Polly DW, Jr., Ledonio CG, Wetjen NM, Larson AN. Accuracy of Pedicle Screw Placement in Children 10 Years or Younger Using Navigation and Intraoperative CT. Clinical spine surgery. 2016;29(3):E135-8.
13. Ohba T, Ebata S, Fujita K, Sato H, Haro H. Percutaneous pedicle screw placements: accuracy and rates of cranial facet joint violation using conventional fluoroscopy compared with intraoperative three-dimensional computed tomography computer navigation. European spine journal : official publication of the European Spine Society, the European Spinal Deformity Society, and the European Section of the Cervical Spine Research Society. 2016;25(6):1775-80.
14. Zhang W, Takigawa T, Wu Y, Sugimoto Y, Tanaka M, Ozaki T. Accuracy of pedicle screw insertion in posterior scoliosis surgery: a comparison between intraoperative navigation and preoperative navigation techniques. European spine journal : official publication of the European Spine Society, the European Spinal Deformity Society, and the European Section of the Cervical Spine Research Society. 2017;26(6):1756-64.
15. Bushberg JT. SJA, Leidholdt E.M., Boone J.M. The Essential Physics of Medical Imaging. Third ed: Lippincott Williams & Wilkins, a WOLTERS KLUWER business; 2012.
16. Christensen DM, Iddins CJ, Sugarman SL. Ionizing radiation injuries and illnesses. Emergency medicine clinics of North America. 2014;32(1):245-65.
17. Fitousi NT, Efstathopoulos EP, Delis HB, Kottou S, Kelekis AD, Panayiotakis GS. Patient and staff dosimetry in vertebroplasty. Spine. 2006;31(23):E884-9; discussioin E90.
18. Graham G.T. CP, Vosper M. Principles of radiological physics. 5th ed. Edinburg: Churchill Livingstone ELSEVIER; 2007. 451 p.
19. Vozenin-Brotons MC. Tissue toxicity induced by ionizing radiation to the normal intestine: understanding the pathophysiological mechanisms to improve the medical management. World journal of gastroenterology. 2007;13(22):3031-2.
20. Do K-H. General Principles of Radiation Protection in Fields of Diagnostic Medical Exposure. Journal of Korean medical science. 2016;31 Suppl 1(Suppl 1):S6-S9.
21. FANC. ARBIS 2017 [Available from: https.//fanc.fgov.be/nl.
22. K Resnick D, Choudhri T, Dailey A, W Groff M, Khoo L, G Matz P, et al. Guideline update for the performance of fusion procedures for degenerative disease of the lumbar spine. Part 1: Introduction and methodology2005. 637-8 p.
23. Taher F, Essig D, Lebl DR, Hughes AP, Sama AA, Cammisa FP, et al. Lumbar degenerative disc disease: current and future concepts of diagnosis and management. Advances in orthopedics. 2012;2012:970752.
24. Wang MY, Henn JS, Mimran RI. Minimally invasive posterior lumbar fusion techniques. Operative Techniques in Neurosurgery. 2004;7(2):64-71.

25. Tanaka M, Sugimoto Y, Arataki S, Takigawa T, Ozaki T. Computer-assisted Minimally Invasive Posterior Lumbar Interbody Fusion without C-arm Fluoroscopy. Acta medica Okayama. 2016;70(1):51-5.
26. Lebl DR. Minimally Invasive Spine Surgery. Current reviews in musculoskeletal medicine. 2017;10(3):407-8.
27. Barrey C, Darnis A. Current strategies for the restoration of adequate lordosis during lumbar fusion2015. 117-26 p.
28. Dewey P, Incoll I. Evaluation of thyroid shields for reduction of radiation exposure to orthopaedic surgeons. The Australian and New Zealand journal of surgery. 1998;68(9):635-6.
29. Mroz TE, Abdullah KG, Steinmetz MP, Klineberg EO, Lieberman IH. Radiation exposure to the surgeon during percutaneous pedicle screw placement. Journal of spinal disorders & techniques. 2011;24(4):264-7.
30. Ul Haque M, Shufflebarger HL, O'Brien M, Macagno A. Radiation exposure during pedicle screw placement in adolescent idiopathic scoliosis: is fluoroscopy safe? Spine. 2006;31(21):2516-20.
31. Villard J, Ryang YM, Demetriades AK, Reinke A, Behr M, Preuss A, et al. Radiation exposure to the surgeon and the patient during posterior lumbar spinal instrumentation: a prospective randomized comparison of navigated versus non-navigated freehand techniques. Spine. 2014;39(13):1004-9.
32. Lian X, Navarro-Ramirez R, Berlin C, Jada A, Moriguchi Y, Zhang Q, et al. Total 3D Airo(R) Navigation for Minimally Invasive Transforaminal Lumbar Interbody Fusion. BioMed research international. 2016;2016:5027340.
33. Navarro-Ramirez R, Lang G, Lian X, Berlin C, Janssen I, Jada A, et al. Total Navigation in Spine Surgery; A Concise Guide to Eliminate Fluoroscopy Using a Portable Intraoperative Computed Tomography 3-Dimensional Navigation System. World neurosurgery. 2017;100:325-35.
34. Hecht N, Kamphuis M, Czabanka M, Hamm B, König S, Woitzik J, et al. Accuracy and workflow of navigated spinal instrumentation with the mobile AIRO® CT scanner. European Spine Journal. 2016;25(3):716-23.
35. Orme NM, Rihal CS, Gulati R, Holmes DR, Lennon RJ, Lewis BR, et al. Occupational Health Hazards of Working in the Interventional Laboratory. Journal of the American College of Cardiology. 2015;65(8):820.
36. Bindal RK, Glaze S, Ognoskie M, Tunner V, Malone R, Ghosh S. Surgeon and patient radiation exposure in minimally invasive transforaminal lumbar interbody fusion. Journal of neurosurgery Spine. 2008;9(6):570-3.
37. Mendelsohn D, Strelzow J, Dea N, Ford NL, Batke J, Pennington A, et al. Patient and surgeon radiation exposure during spinal instrumentation using intraoperative computed tomography-based navigation. The spine journal : official journal of the North American Spine Society. 2016;16(3):343-54.
38. Chan VO, McDermott S, Buckley O, Allen S, Casey M, O'Laoide R, et al. The Relationship of Body Mass Index and Abdominal Fat on the Radiation Dose Received During Routine Computed Tomographic Imaging of the Abdomen and Pelvis. Canadian Association of Radiologists Journal. 2012;63(4):260-6.
39. Bourgeois AC, Faulkner AR, Pasciak AS, Bradley YC. The evolution of image-guided lumbosacral spine surgery. Annals of translational medicine. 2015;3(5):69-.
40. Meng XT, Guan XF, Zhang HL, He SS. Computer navigation versus fluoroscopy-guided navigation for thoracic pedicle screw placement: a meta-analysis. Neurosurgical review. 2016;39(3):385-91.
41. Lian X, Navarro-Ramirez R, Berlin C, Jada A, Moriguchi Y, Zhang Q, et al. Total 3D Airo® Navigation for Minimally Invasive Transforaminal Lumbar Interbody Fusion. BioMed research international. 2016;2016:5027340-.
42. Peersman G, Laskin R, Davis J, Peterson MGE, Richart T. Prolonged operative time correlates with increased infection rate after total knee arthroplasty. HSS J. 2006;2(1):70-2.
43. Waschke A, Walter J, Duenisch P, Reichart R, Kalff R, Ewald C. CT-navigation versus fluoroscopy-guided placement of pedicle screws at the thoracolumbar spine: single center experience of 4,500 screws. European spine journal : official publication of the European Spine Society, the European Spinal Deformity Society, and the European Section of the Cervical Spine Research Society. 2013;22(3):654-60.
44. Noriega DC, Hernández-Ramajo R, Rodríguez-Monsalve Milano F, Sanchez-Lite I, Toribio B, Ardura F, et al. Risk-benefit analysis of navigation techniques for vertebral transpedicular instrumentation: a prospective study. The Spine Journal. 2017;17(1):70-5.

Supplementary figures

Clinical efficacy:

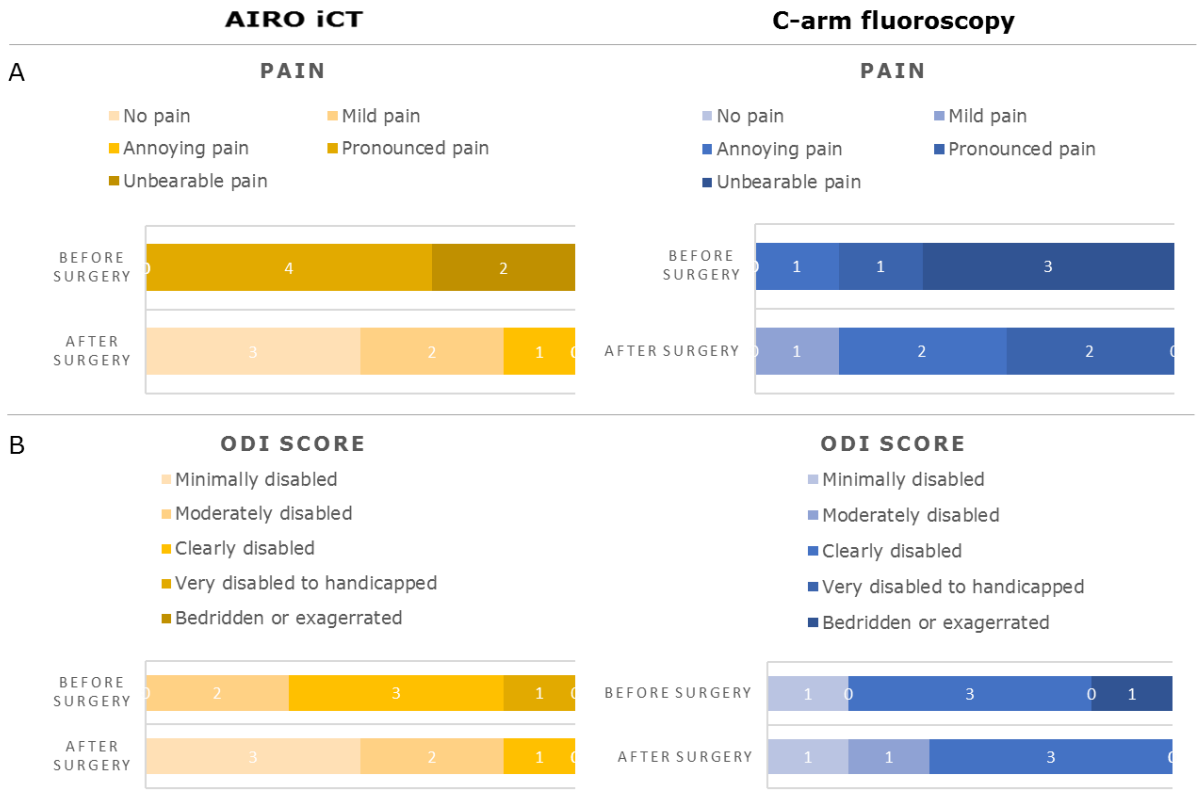

Supplementary figure 1: Pain and disability score after a postoperative period of six months to two years. *A) Pain degree of the study participants before surgery and after a postoperative period of six months to two years surgery with AIRO iCT (left) (n=6) or C-arm fluoroscopy (right) (n=5). Data were obtained by a numeric visual analog scale. B) ODI score of the study participants before surgery and six weeks after surgery with AIRO iCT (left) (n=6) or C-arm fluoroscopy (right) (n=5).Data were analyzed by an ODI questionnaire. iCT: intraoperative computed tomography; ODI: Oswestry disability index.*

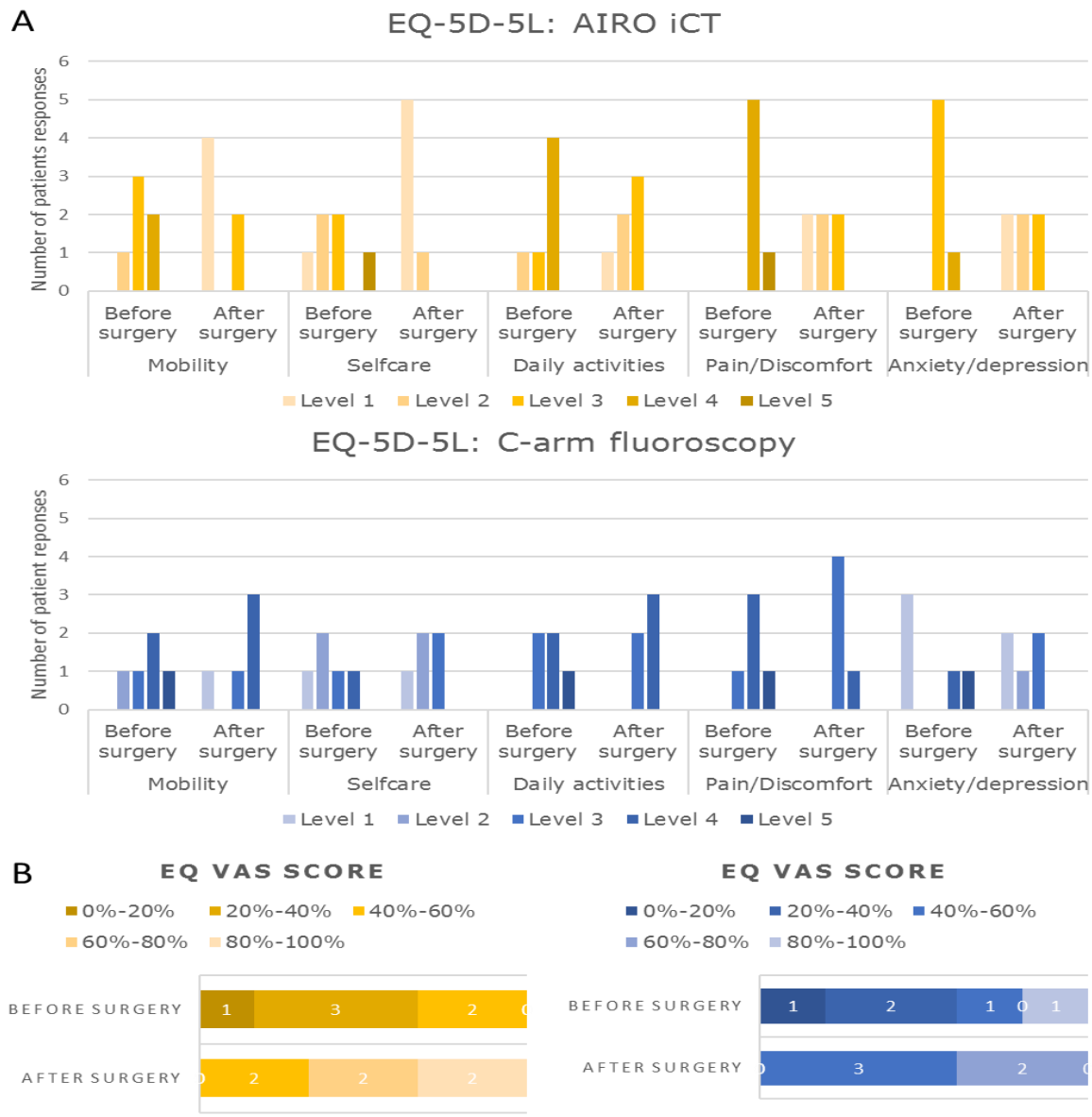

Supplementary *figure 2: Health state score after a postoperative period of six months to two years.* *The health state of the study participants was evaluated before the surgery and after a period of six postoperative months to two years with an EQ-5D-5L questionnaire and an EQ-VAS. A) Scoring of the five dimensions of health state (mobility, self-care, daily activities, pain/discomfort, and anxiety/depression) before and after surgery with iCT (yellow) (n=6) or C-arm fluoroscopy (blue) (n=5). Level 1= no problems or no pain/discomfort, anxiety/depression, Level 2= mild problems or mild pain/discomfort, anxiety/depression, Level 3= Moderated problems or moderate pain/discomfort, anxiety/depression, Level 4= severe problems or severe pain/discomfort, anxiety/depression, Level 5= extreme problems or extreme pain/discomfort, anxiety /depression. B) The self-rated health score of the study patients before and after surgery with AIRO iCT (left) (n=6) or C-arm fluoroscopy (right) (n=5). EQ-5D-5L: EuroQol- five dimensions- 5 levels; iCT: intraoperative computed tomography; VAS: visual analog scale.*